Supporting Information

Novel Psoralen Derivatives as Anti-Breast Cancer Agents: Synthesis and Evaluation of Dark and Light-Activated Cytotoxicity

Chiphada Aekrungrueangkit[1], Sirilak Wangngae[2], Anyanee Kamkaew[2], Ruchuta Ardkhean[3], Jutatip Boonsombat[4,5,*], Somsak Ruchirawat[4,5,6], Tanatorn Khotavivattana[1,*]

[1] *Center of Excellence in Natural Products Chemistry, Department of Chemistry, Faculty of Science, Chulalongkorn University, Bangkok, 10330, Thailand*

[2] *School of Chemistry, Institute of Science, Suranaree University of Technology, Nakhon, Ratchasima, 30000, Thailand.*

[3] *Princess Srisavangavadhana College of Medicine, Chulabhorn Royal Academy, Bangkok, 10210, Thailand*

[4] *Chulabhorn Research Institute, Bangkok, 10330, Thailand*

[5] *Center of Excellence on Environmental Health and Toxicology (EHT), OPS, MHESI, Thailand*

[6] *Program in Chemical Sciences, Chulabhorn Graduate Institute, Chulabhorn Royal Academy, Bangkok 10210, Thailand*

**Corresponding authors* *jutatip@cri.or.th* *and* *tanatorn.k@chula.ac.th*

Content

1. Chemoprevention activity

1.1. Scavenging of diphenyl-picryl-hydrazyl radicals (DPPH)

Radical scavenging potential was performed by reaction with 1,1-diphenyl-2-picrylhydrazyl (DPPH) free radicals as described by van Amsterdam et al., 1992.[i] Ascorbic acid was used as the reference compound, showing a half-maximal scavenging concentration (IC_{50}) at 43.1 ± 1.3 µM (**Table S1**).

1.2. Inhibition of 12-*O*-tetradecanoylphorbol-13-acetate (TPA)-induced superoxide anion radical generation in differentiated HL-60 cells (HL-60 Antioxidant)

TPA-induced superoxide anion radical formation was detected in differentiated HL-60 cells by photometric determination of cytochrome c reduction as previously described by Gerhäuser et al., 2003.[ii] Superoxide dismutase (SOD;15U) was a positive control. Only the test compounds with >50% cell viability were considered to be evaluated for the scavenging potential (**Table S1**).

1.3. Inhibition of superoxide radical formation by xanthine/xanthine oxidase (XXO)

Inhibition of superoxide radical formation was detected indirectly by measuring the rate of reduced XTT production as described by Gerhäuser et al, 2003.[iii] Gallic acid was a positive control, exhibiting an IC_{50} value of 2.8 ± 0.1 µM. Inhibition of superoxide radical formation was determined only when the tested compounds did not inhibit xanthine oxidase (**Table S1**).

1.4. Inhibition of xanthine oxidase (IXO)

Xanthine oxidase activity was determined by quantifying the amount of uric acid produced from xanthine. The method was followed as described by Rangkadilok et al., 2007.[iii] Allopurinol was used as a positive control, inhibiting xanthine oxidase activity with an IC_{50} value of 3.8 ± 0.4 µM (**Table S1**).

1.5. Inhibition of lipoxygenase (LOX)

Lipoxygenase activity was performed by measuring leukotriene metabolite as described by Gleason et al., 1995.[iv] Nordihydroquaiaretic acid, a positive compound, inhibited lipoxygenase activity with an IC_{50} value of 3.8 ± 0.6 µM (**Table S1**).

Table S1 Chemoprevention evaluation of psoralen derivatives.

Comp.	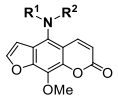		DPPH		HL-60 Antiox.		XXO		IXO		LOX	
	R^1	R^2	%Inh	IC_{50} [μM]	%Inh	IC_{50} [μM]	%Inh	IC_{50} [μM]	%Inh	IC_{50} [μM]	%Inh	IC_{50} [μM]
8-MOP		-H	1	-	17	-	37	-	-	183.7 ± 5.4	9	-
1		$-NO_2$	5	-	1	-	IX	-	HBg, HOD	-	4	-
2		$-NH_2$	23	-	0	-	IX	-	HBg, HOD	-	3	-
3a	H		6	-	3	-	IX	-	HBg, HOD	-	0	-
3b	H	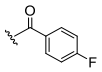	3	-	1	-	IX	-	HBg, HOD	-	3	-
3c	H	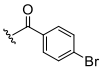	6	-	Toxic	-	25	-	HBg, HOD	-	4	-
3d	H	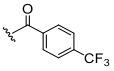	7	-	Toxic	-	IX	-	HBg, HOD	-	2	-
3e	H	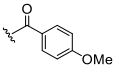	4	-	0	-	IX	-	HBg, HOD	-	0	-
3f	H	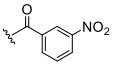	1	-	7	-	33	-	HOD	-	0	-
3g	H		3	-	17	-	IX	-	HOD	-	3	-
3h	H		6	-	24	-	IX	-	HOD	-	5	-
3i	H		1	-	11	-	IX	-	47	-	4	-
3j	H		2	-	11	-	-	187.3 ± 23.3	29	-	6	-
3k	H		2	-	11	-	-	394.4 ± 65.8	17	-	0	-
3l	H		1	-	10	-	IX	-	HOD	-	6	-
3m	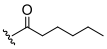	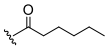	1	-	0	-	2	-	HOD	-	-	56.1 ± 0.5
3n	H		1	-	8	-	47	-	HBg, HOD	-	6	-
4a	H		-	145.0 ± 9.6	7	-	34	-	-	27.4 ± 5.9	30	-
4b	H	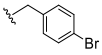	-	165.7 ± 1.1	Toxic	-	HBg	-	HBg	-	9	-
5	H		8	-	32	-	-	90.7 ± 6.2	21%	-	2	-
6	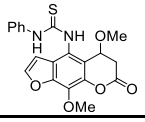		-	52.6 ± 3.1	Toxic	-	24	-	48, HOD	-	16	-
Screening Concentration (final conc.)			250 μM		100 μM		500 μM		500 μM		100 μM	
Standard			Ascorbic acid 43.1 ± 1.3 μM		Superoxide dismutase		Gallic acid 2.8 ± 0.1 μM		Allopurinol 3.8 ± 0.4 μM		Nordihydroquaiaretic acid 3.8 ± 0.6 μM	

%Inhibition at tested concentration, - = not determined, HBg = high background, HOD = High optical density (absorbance > 1), IX = Inhibit xanthine oxidase, Toxic = tested compound was toxic with cell (cannot detect the generated radical).

2. Molecular docking results of selected compounds

Table S2 Docking scores, protein residues with hydrogen-bond, halogen bond, Pi-cation, Pi-Pi stacking or hydrophobic interactions with the ligands, and phototoxicity of selected compounds.

Comp.	SK-BR-3[a] with UVA light (2.0 J/cm^2)	HER2 (PDB ID: 3PP0)		
	IC_{50} (μM)	RMSD[b] (Å)	Docking scores[c] (kcal/mol)	Protein residues[c]
8MOP	24.66 ± 3.02	4.65	-7.9	-
3e	66.72 ± 2.75	0.06	-7.2	ARG849, PHE731
3g	2.71 ± 0.84	0.51	-9.4	MET801
3j	3.05 ± 1.02	0.04	-8.3	MET801, ASP863
3k	66.09 ± 5.21	0.49	-8.4	MET801
3l	48.14 ± 3.07	0.03	-8.5	MET801
3m	27.09 ± 1.20	0.22	-6.0	ARG849
03Q[d]	-	0.07	-11.5	MET801, Lys753, Leu796

[a]HER2 mammary carcinoma; [b]RMSD between docked poses obtained from two grid boxes [box1; center at (10,29,27), x = 28 Å, y = 40 Å, z = 20 Å, and box 2; center at (9,24.5,42) x = 28 Å, y = 48 Å, z = 44 Å]; [c]Box 1, [d]Co-crystallized ligand of 3PP0.

3. Light-activated cytotoxicity of psoralen derivatives against SK-BR-3

Light-activated cytotoxicity of psoralen derivatives against SK-BR-3 in the different concentration under irradiation with UVA (2 J/cm^2) for 12.5 min.

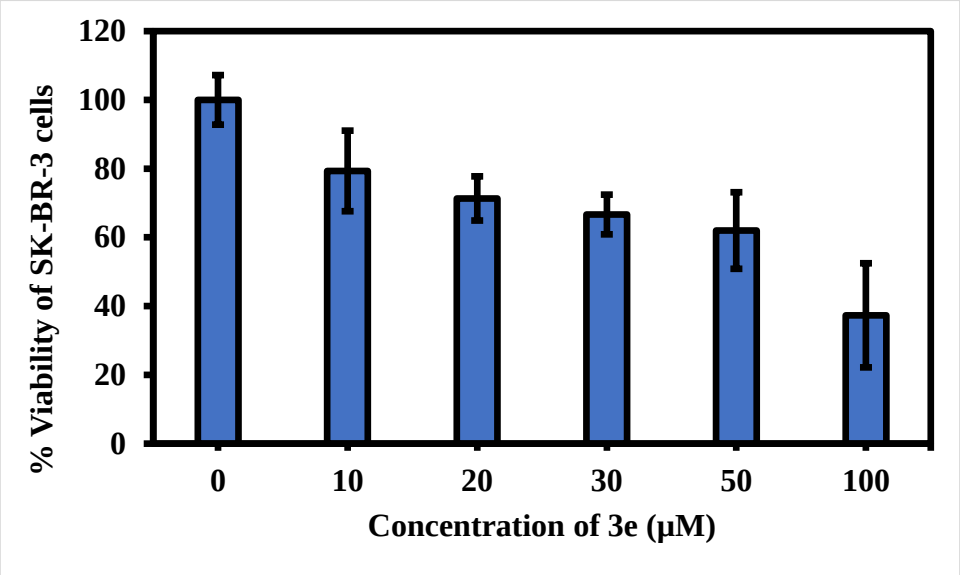

Figure S1 The IC_{50} determination of **3e**

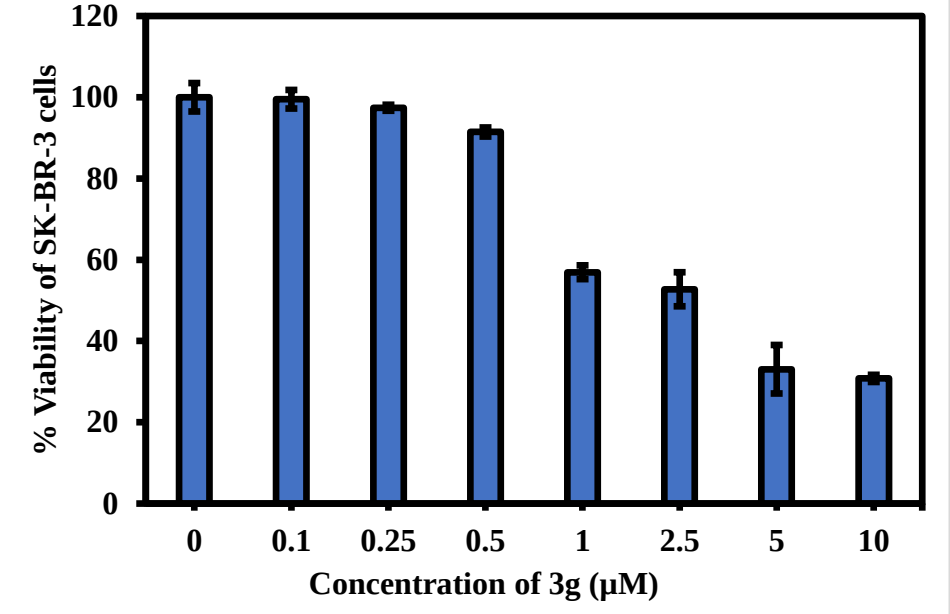

Figure S2 The IC_{50} determination of **3g**

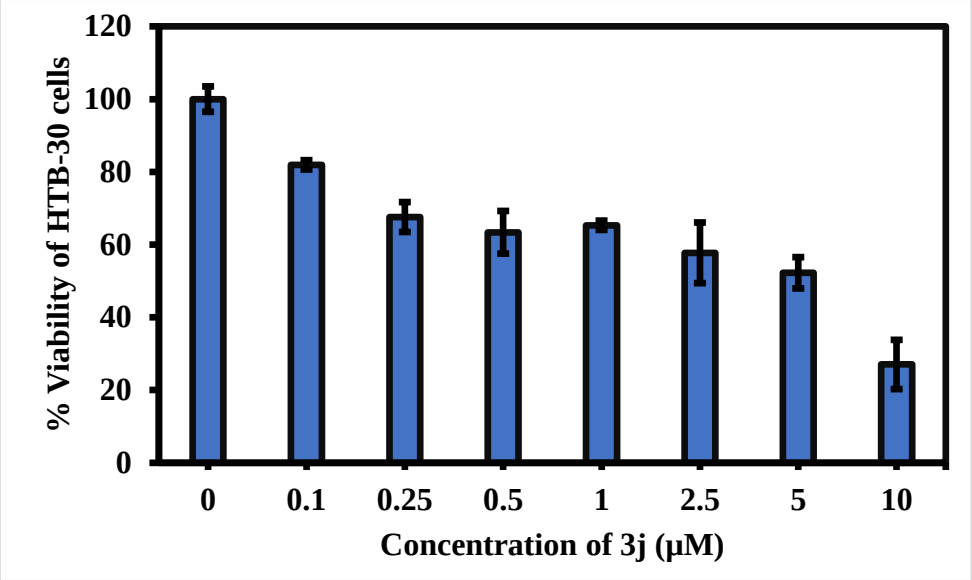

Figure S3 The IC_{50} determination of **3j**

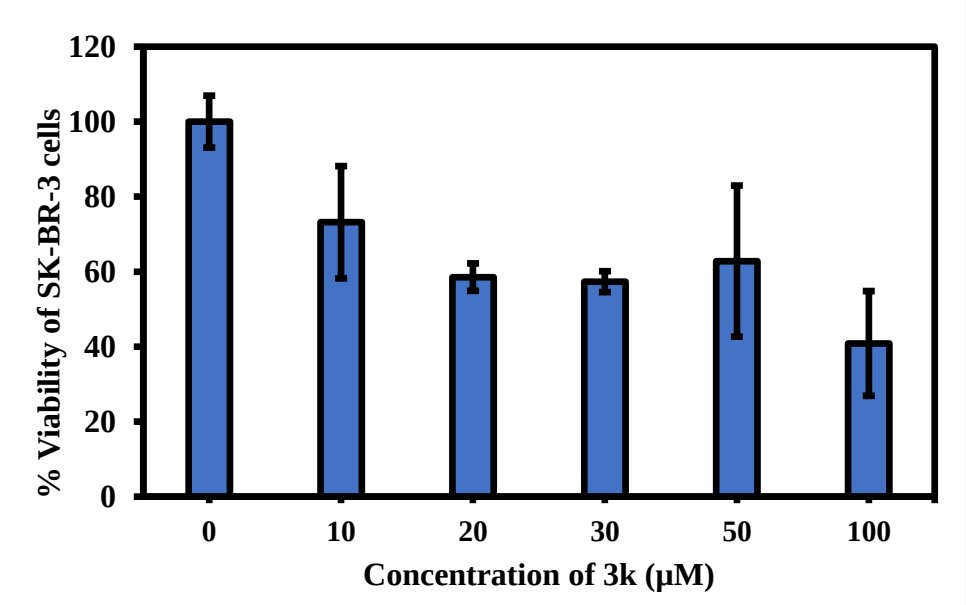

Figure S4 The IC_{50} determination of **3k**

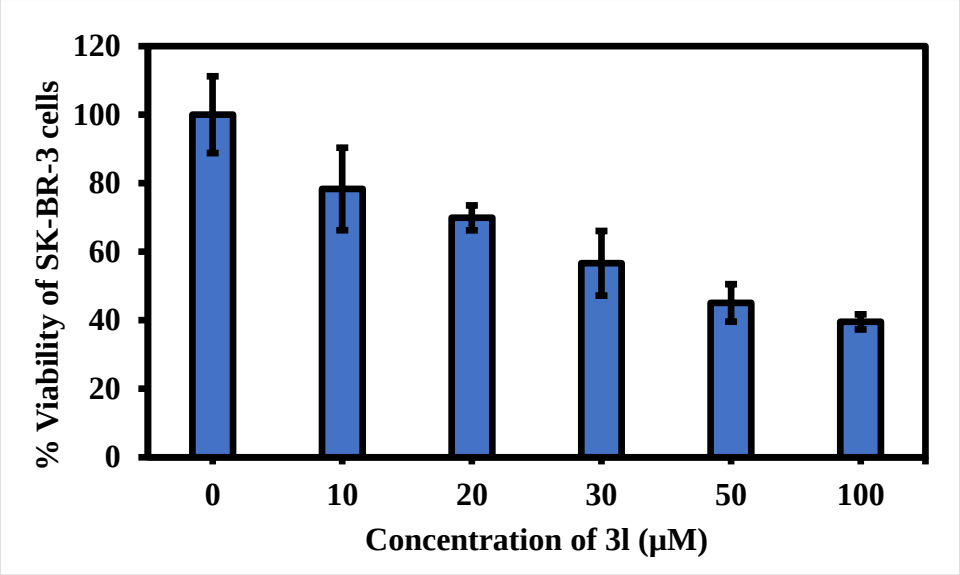

Figure S5 The IC_{50} determination of **3l**

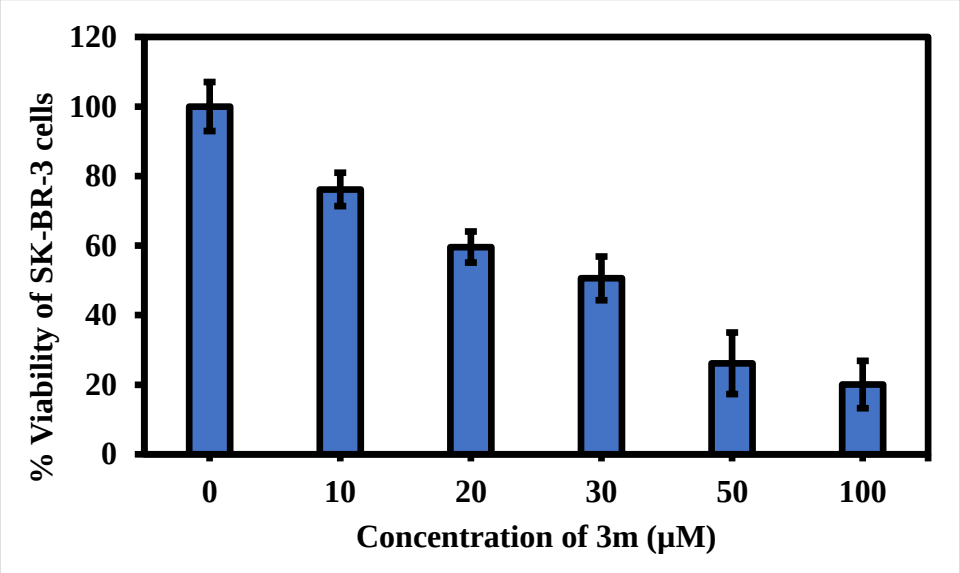

Figure S6 The IC_{50} determination of **3m**

4. NMR and HRMS spectra

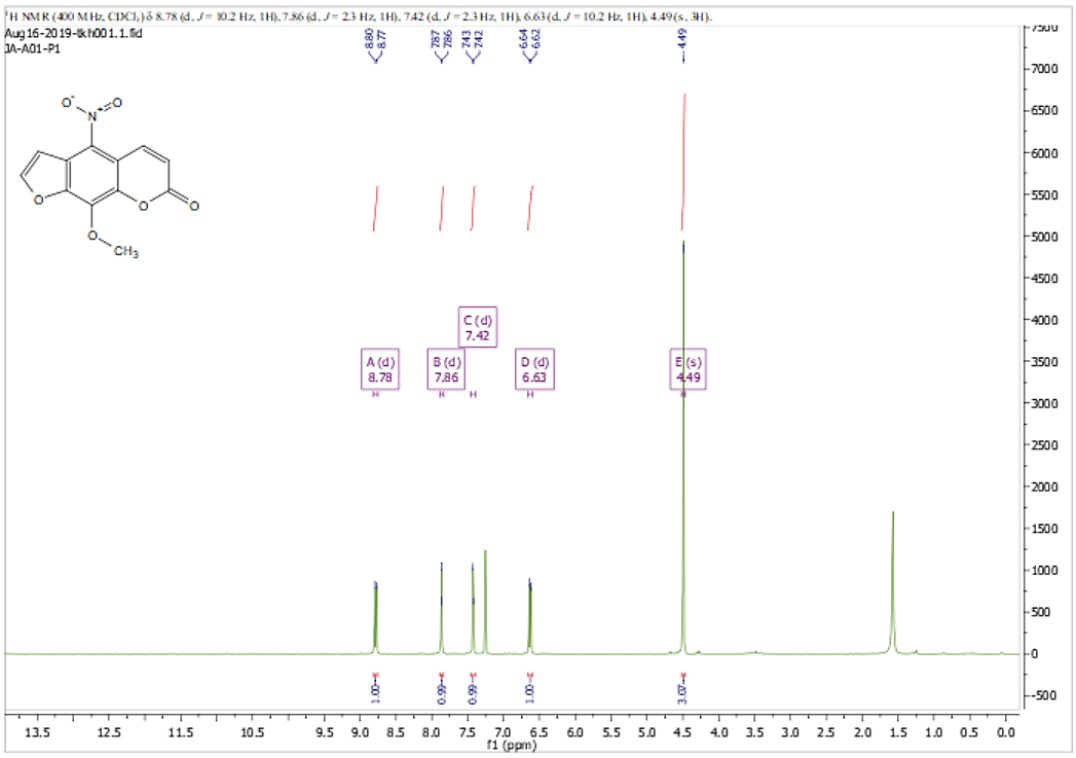

Figure S7 ^{1}H NMR spectrum of **1**

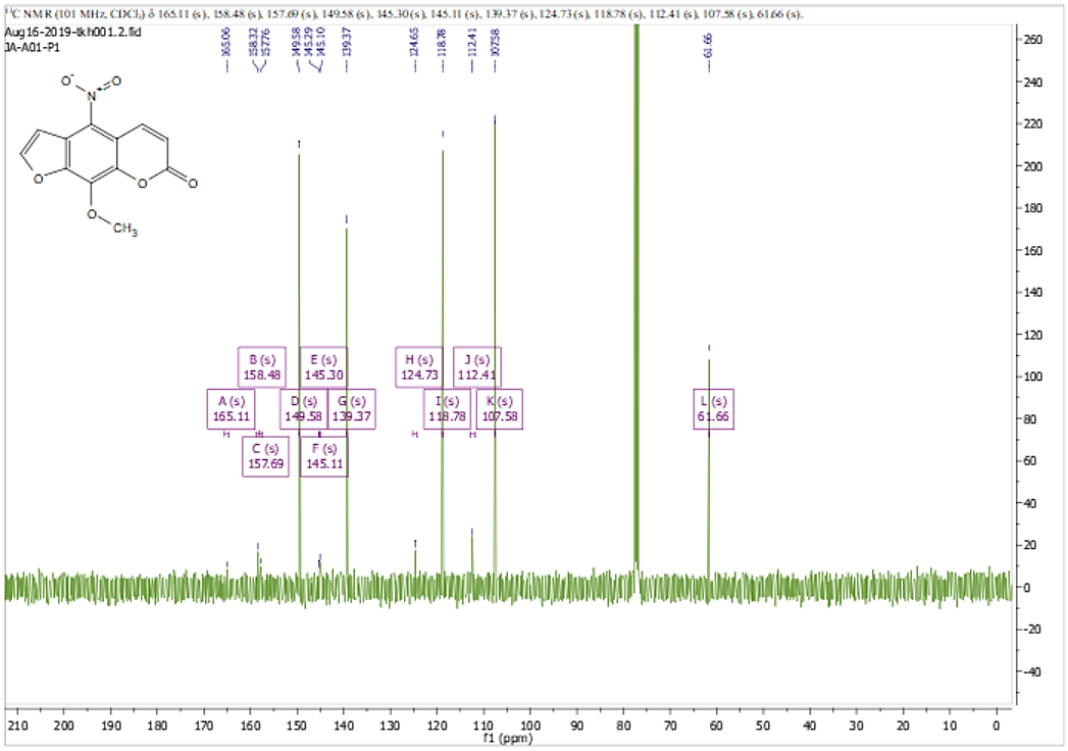

Figure S8 ^{13}C NMR spectrum of **1**

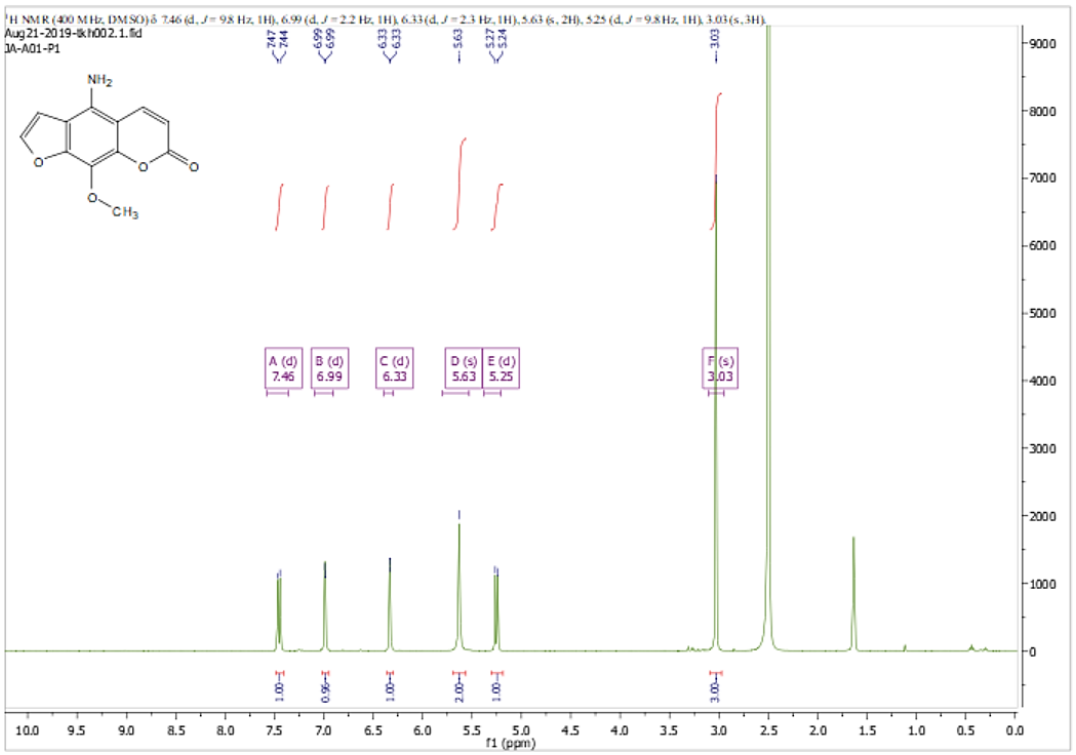

Figure S10 ^{1}H NMR spectrum of **2**

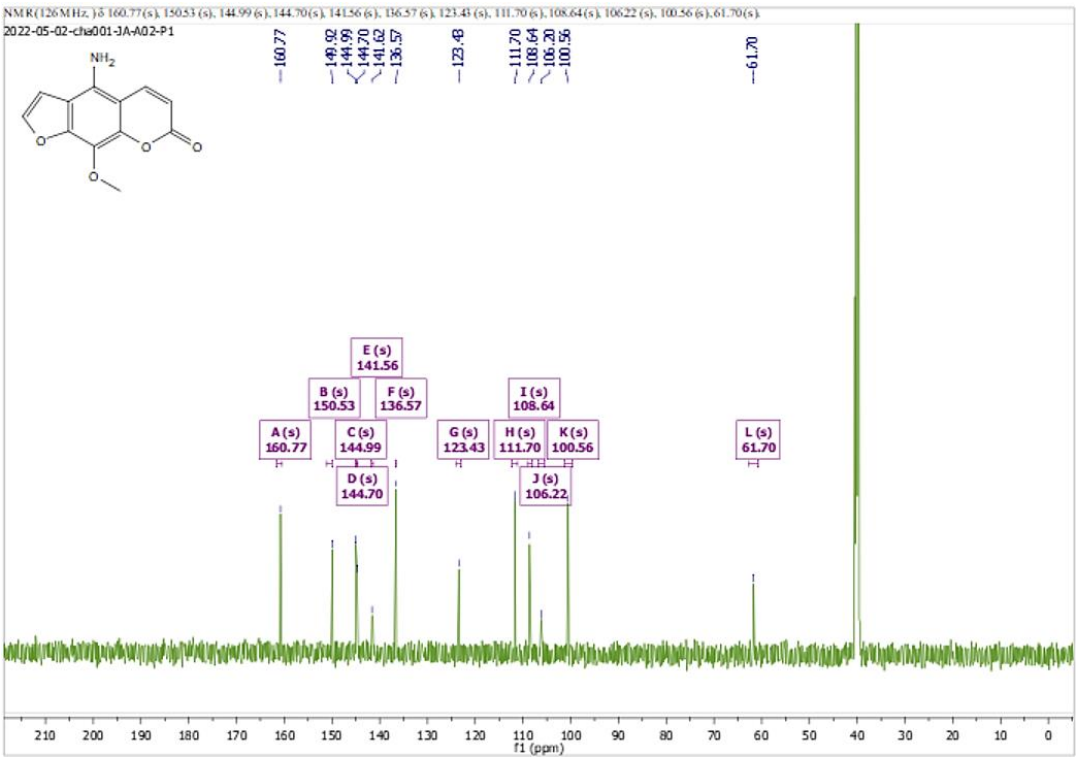

Figure S11 ^{13}C NMR spectrum of **2**

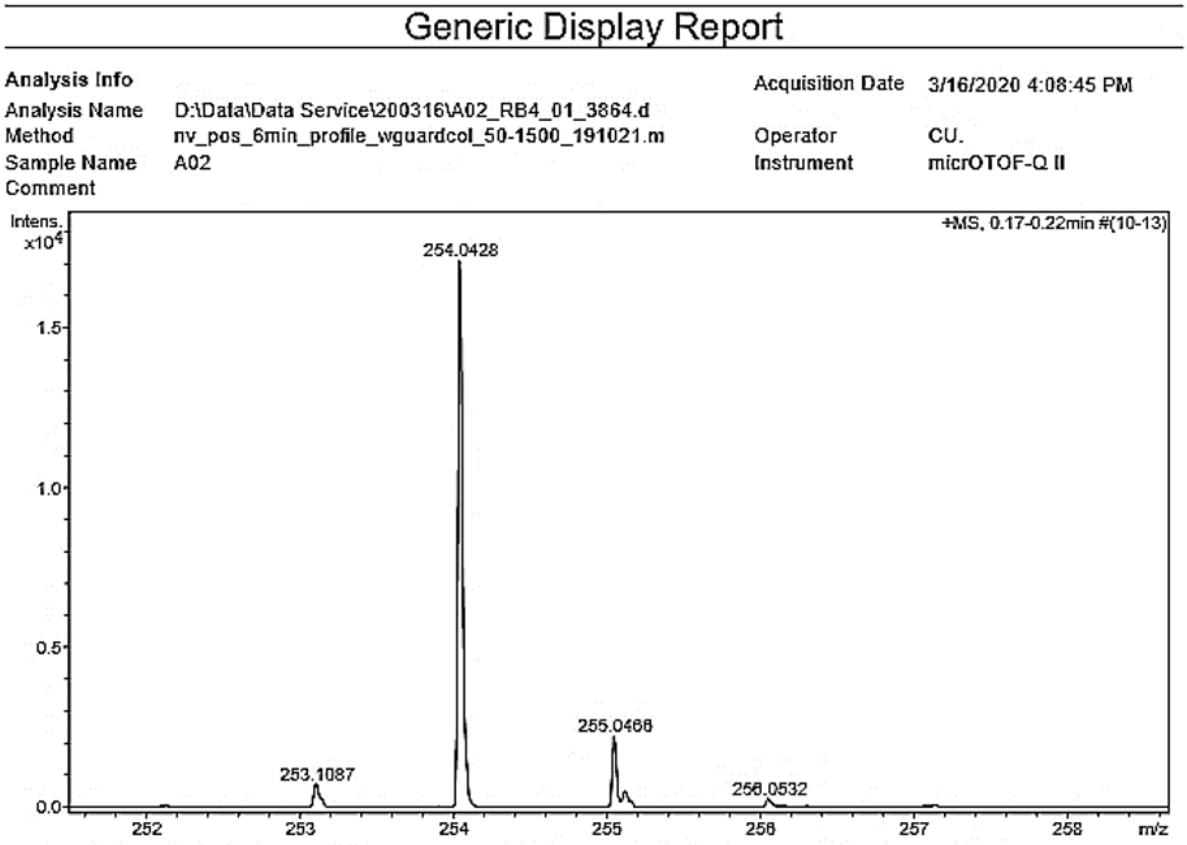

Figure S12 HRMS spectrum of **2**

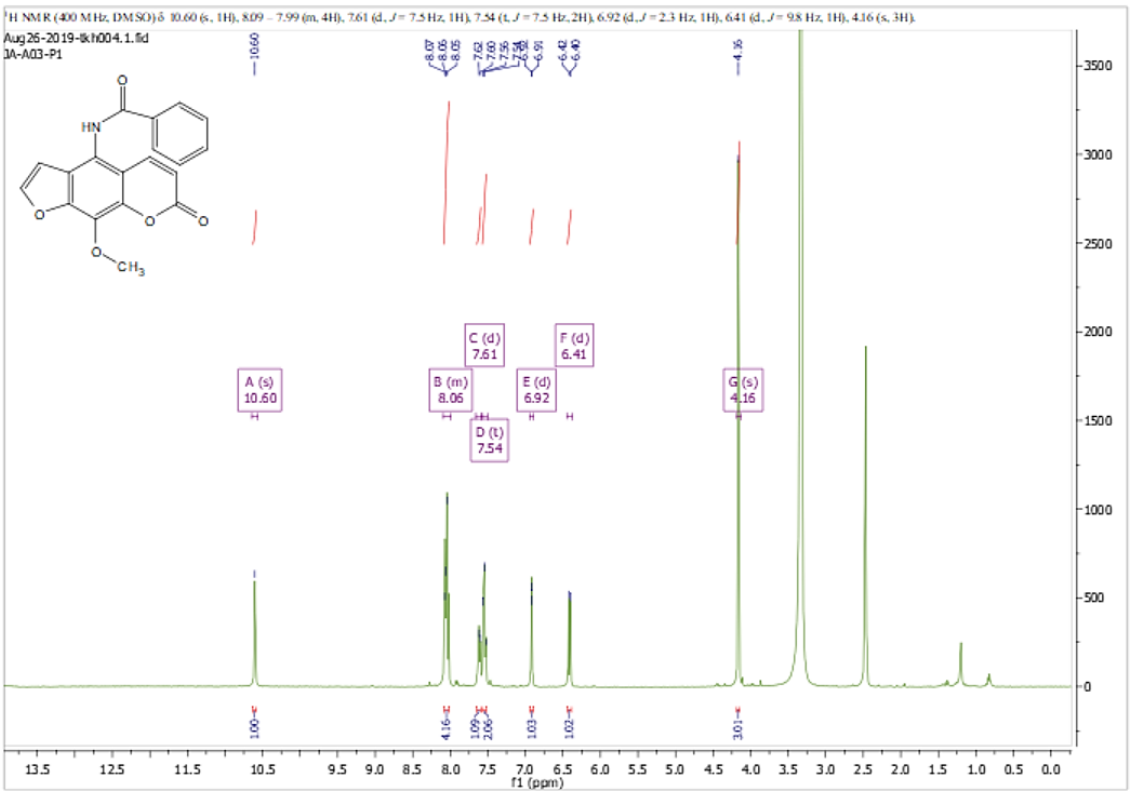

Figure S13 ^{1}H NMR spectrum of **3a**

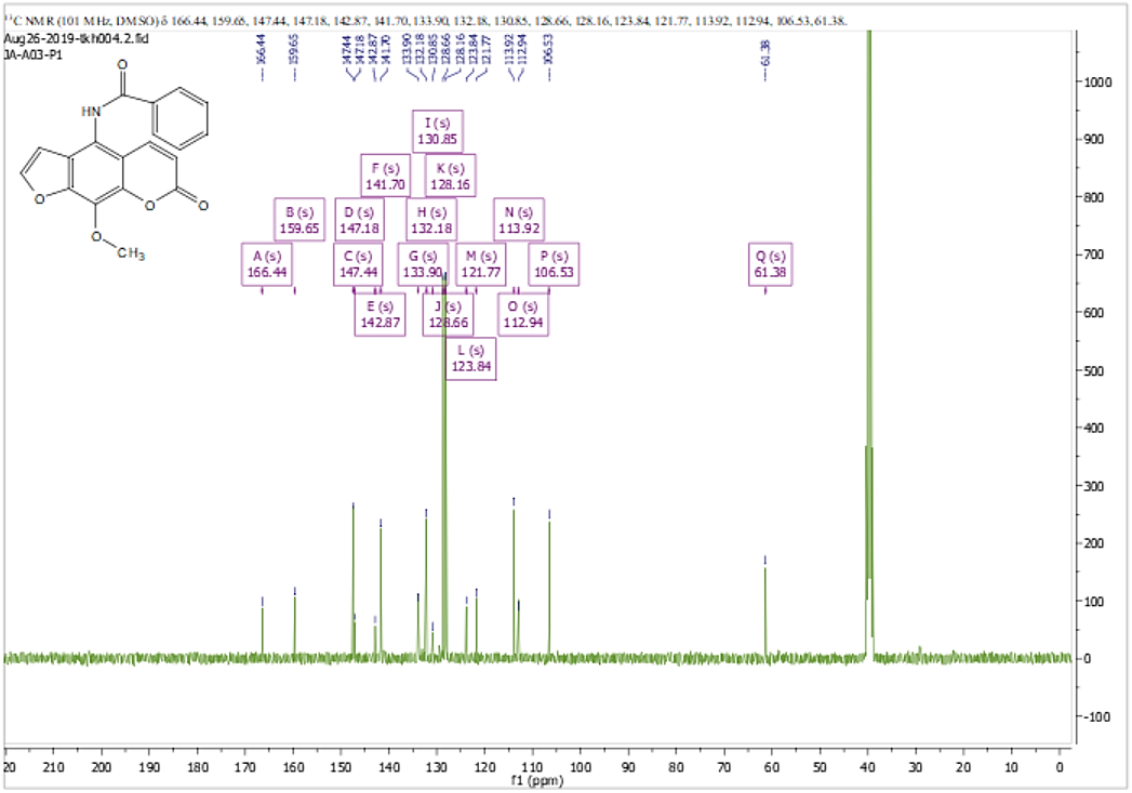

Figure S14 ^{13}C NMR spectrum of **3a**

Generic Display Report

Analysis Info

Analysis Name	D:\Data\Data Service\200316\A03_RB5_01_3867.d	Acquisition Date	3/16/2020 4:28:10 PM
Method	nv_pos_6min_profile_wguardcol_50-1500_191021.m	Operator	CU.
Sample Name	A03	Instrument	micrOTOF-Q II
Comment			

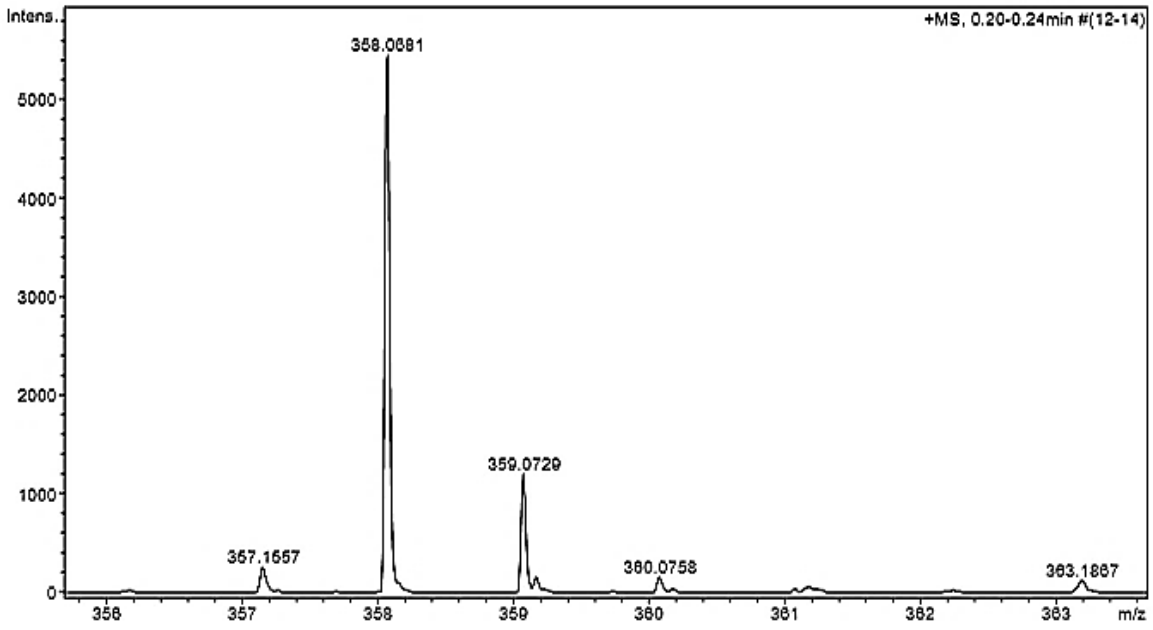

Figure S15 HRMS spectrum of **3a**

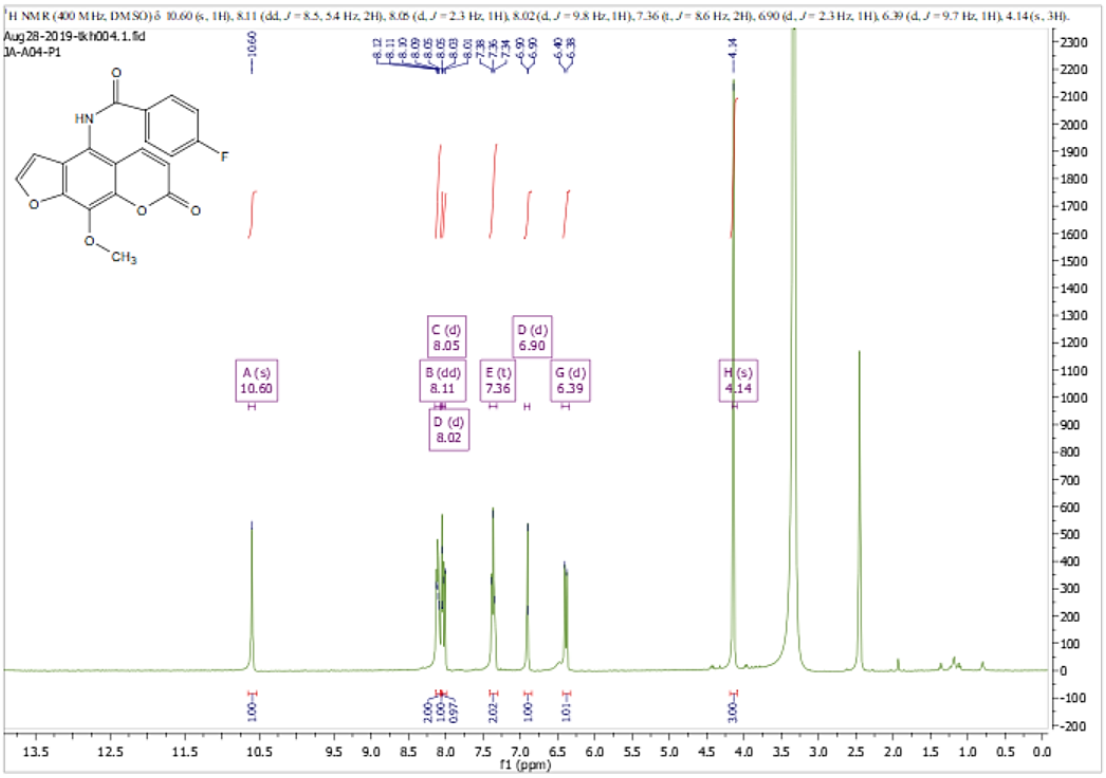

Figure S16 ^{1}H NMR spectrum of **3b**

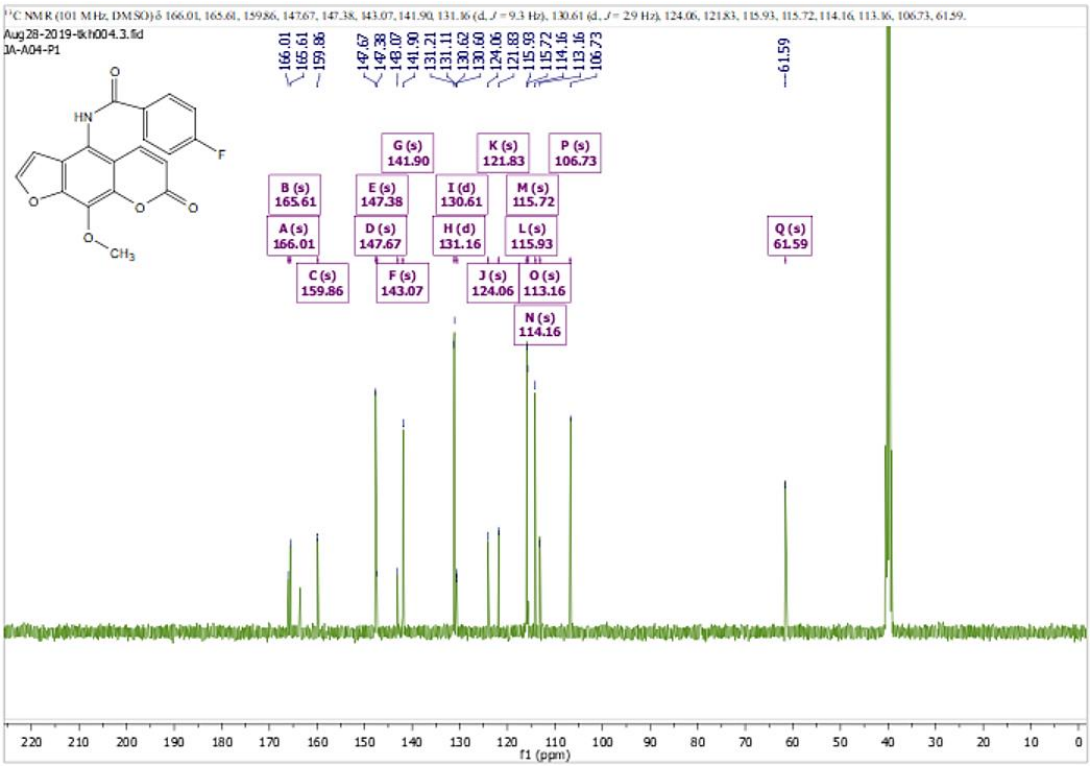

Figure S17 ^{13}C NMR spectrum of **3b**

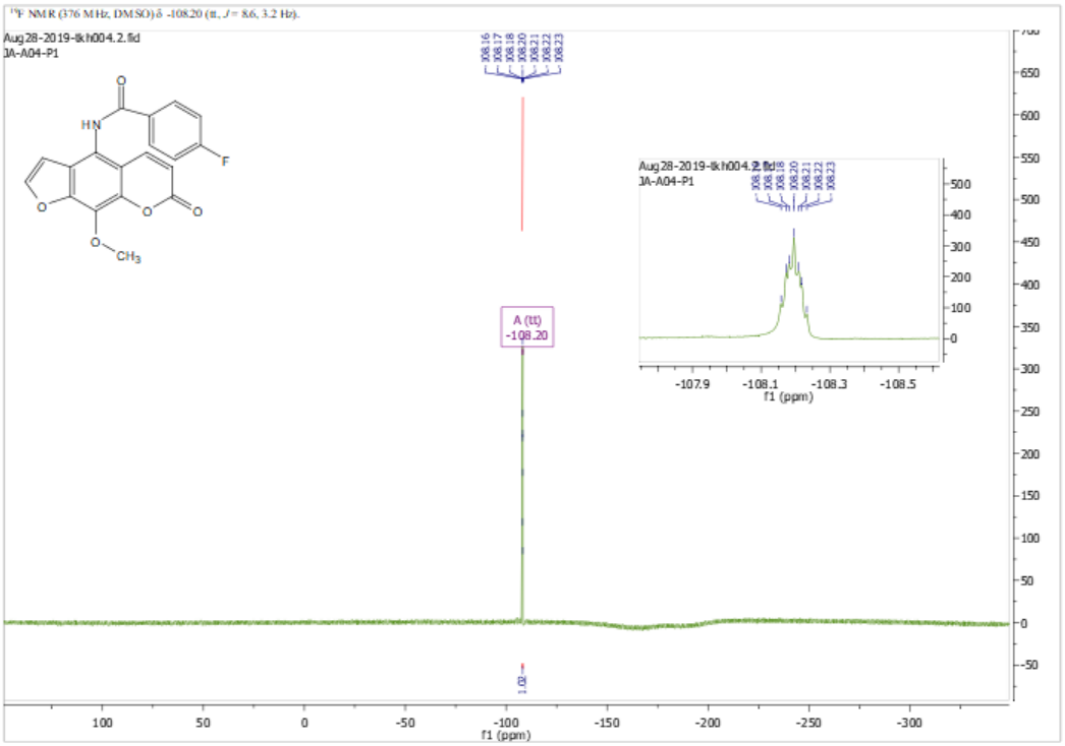

Figure S18 ^{19}F NMR spectrum of **3b**

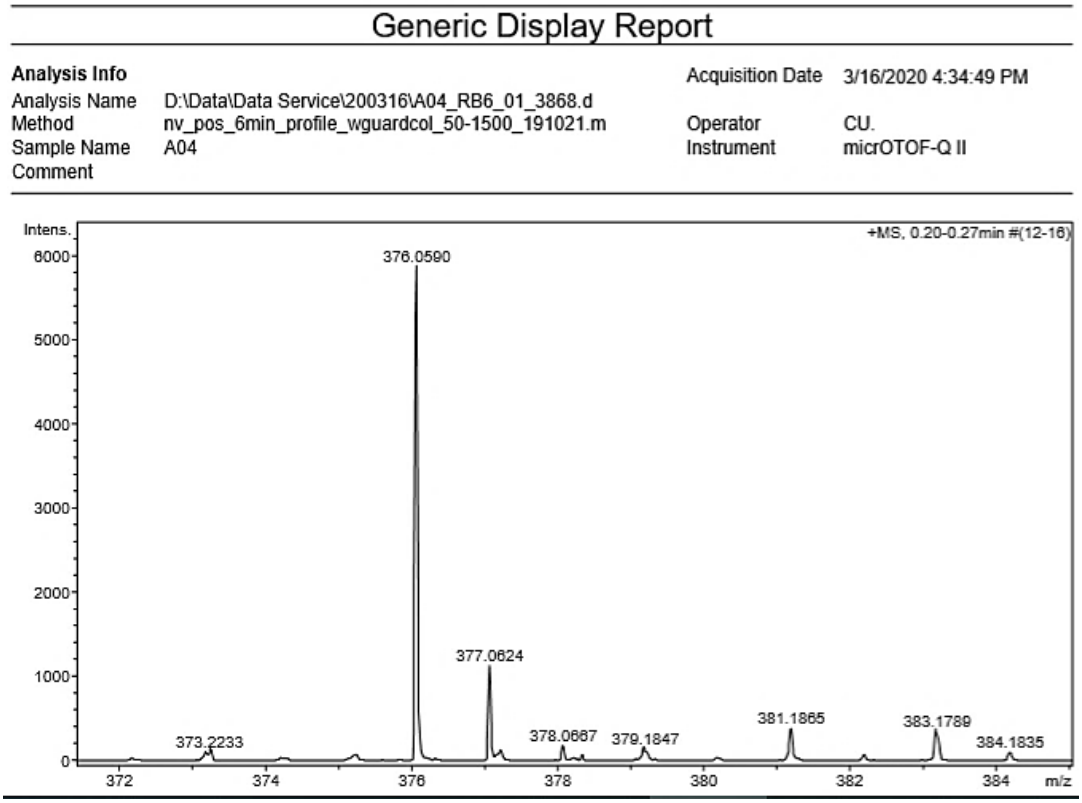

Figure S19 HRMS spectrum of **3b**

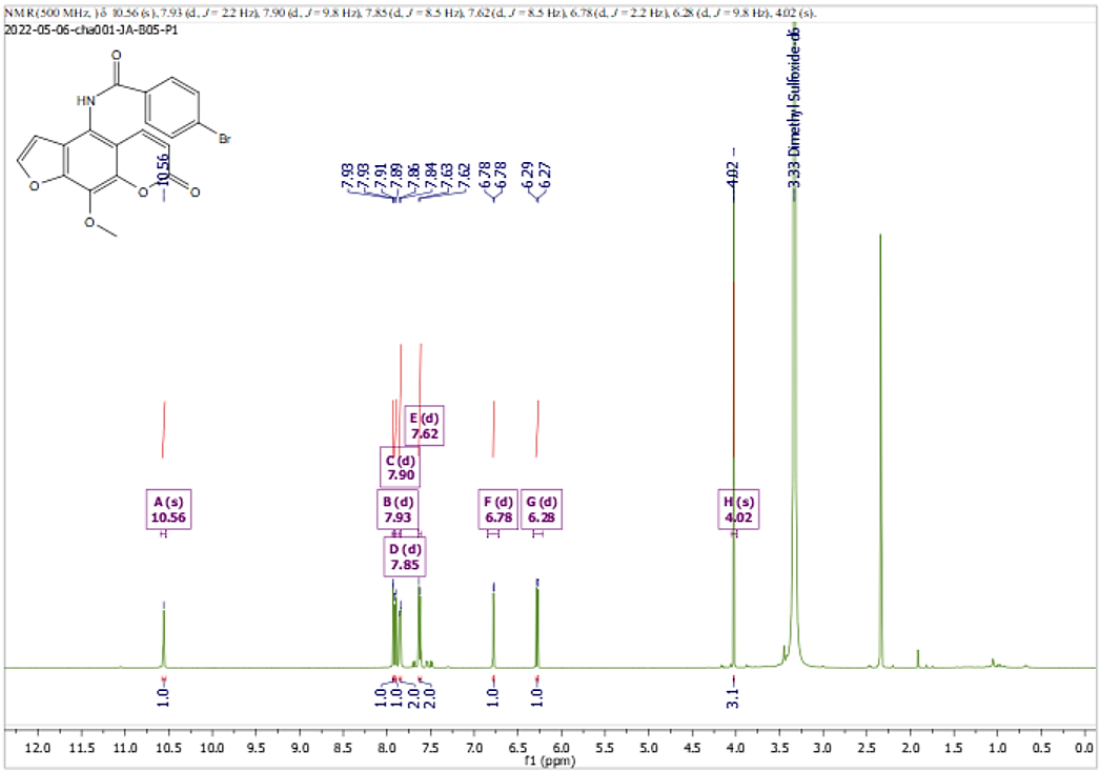

Figure S20 ^{1}H NMR spectrum of **3c**

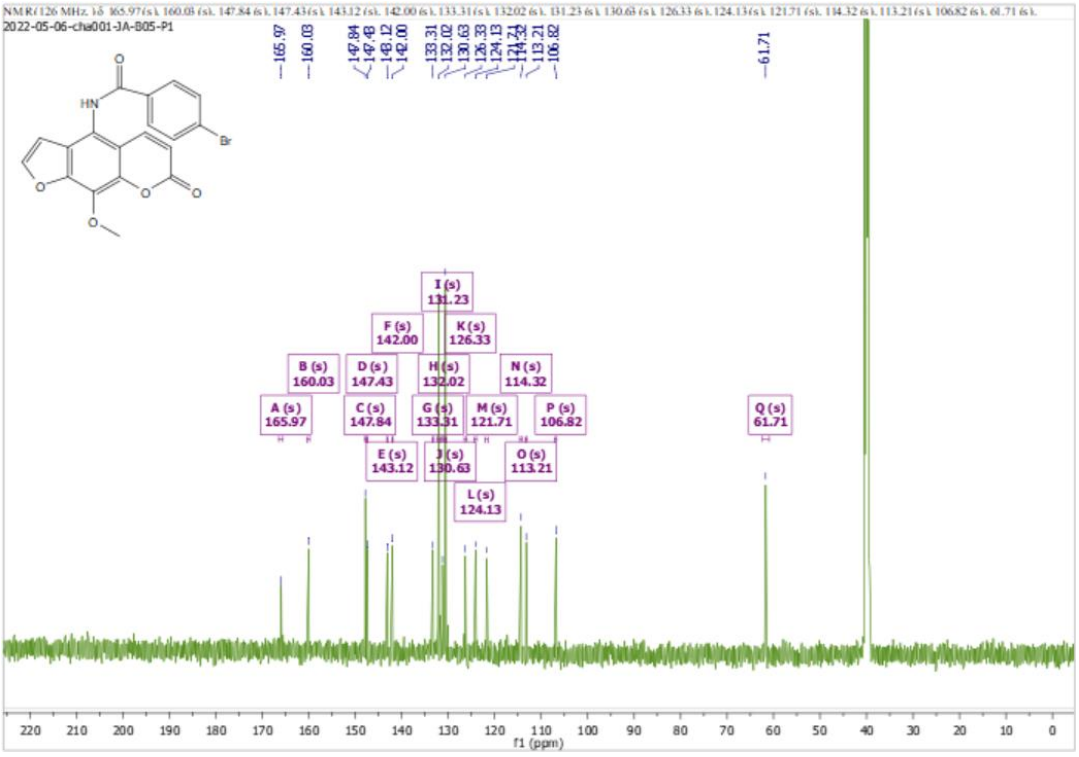

Figure S21 ^{13}C NMR spectrum of **3c**

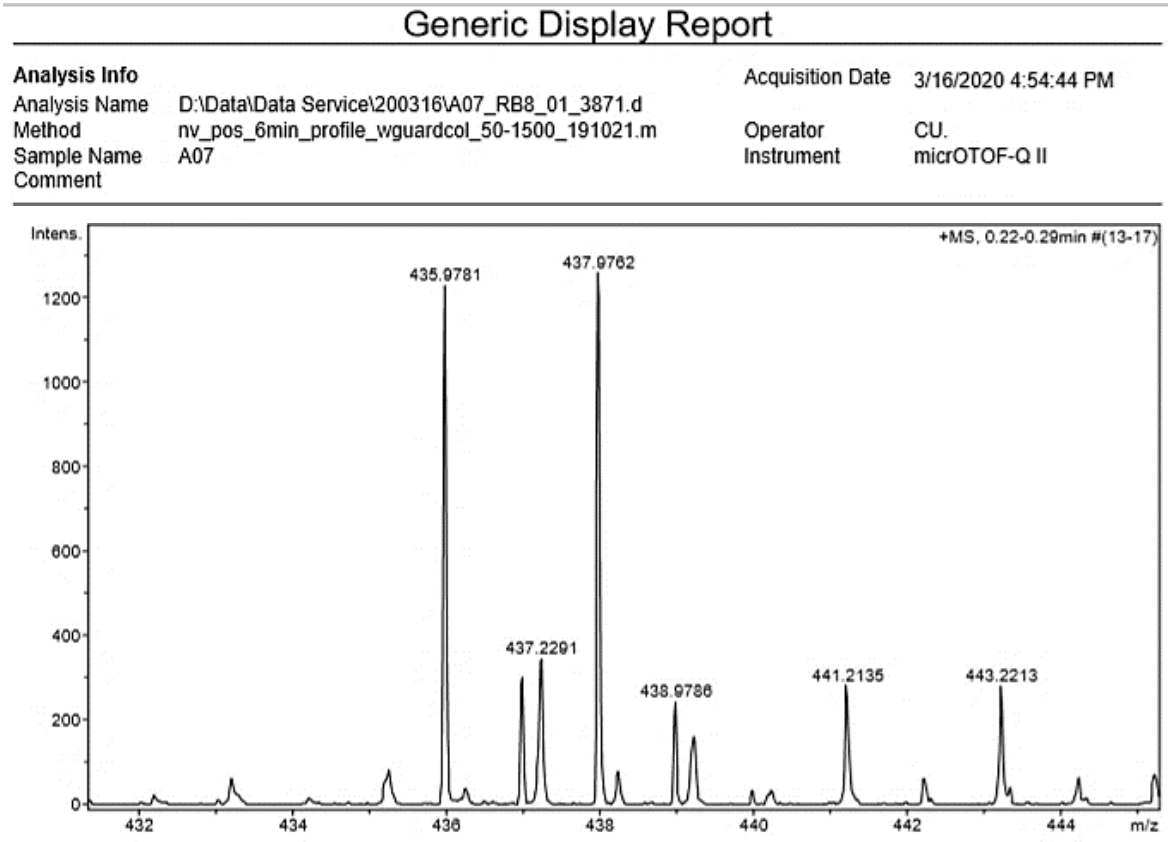

Figure S22 HRMS spectrum of **3c**

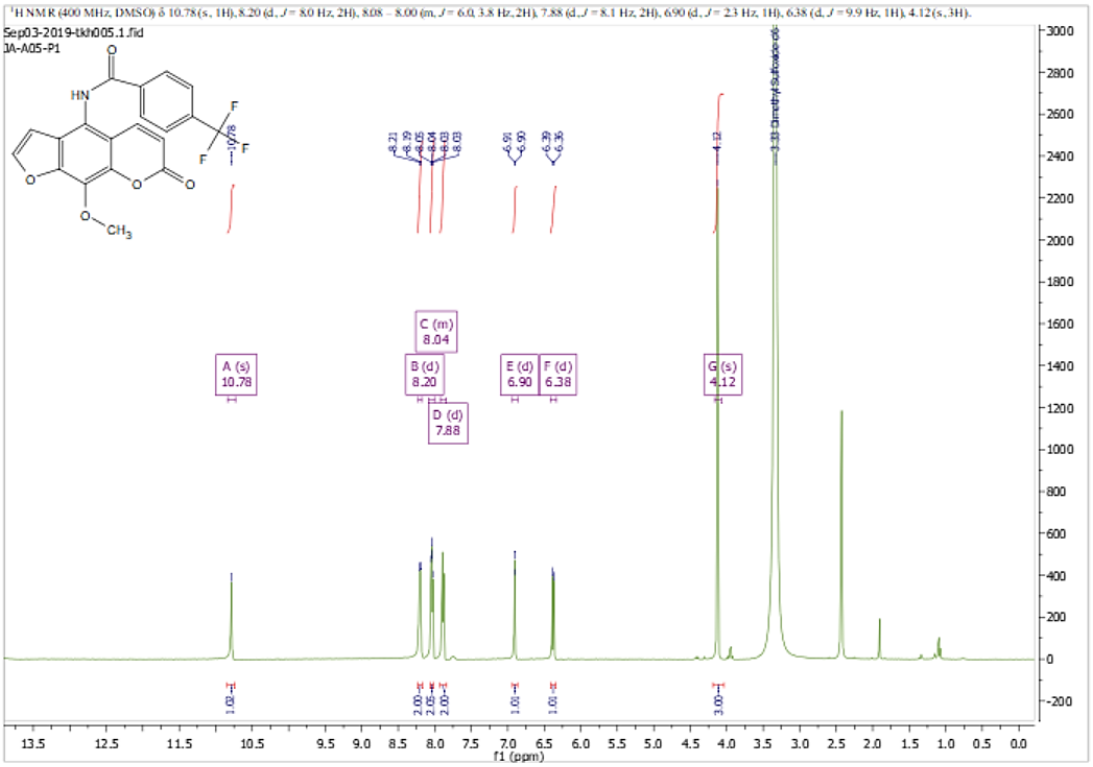

Figure S23 ^{1}H NMR spectrum of **3d**

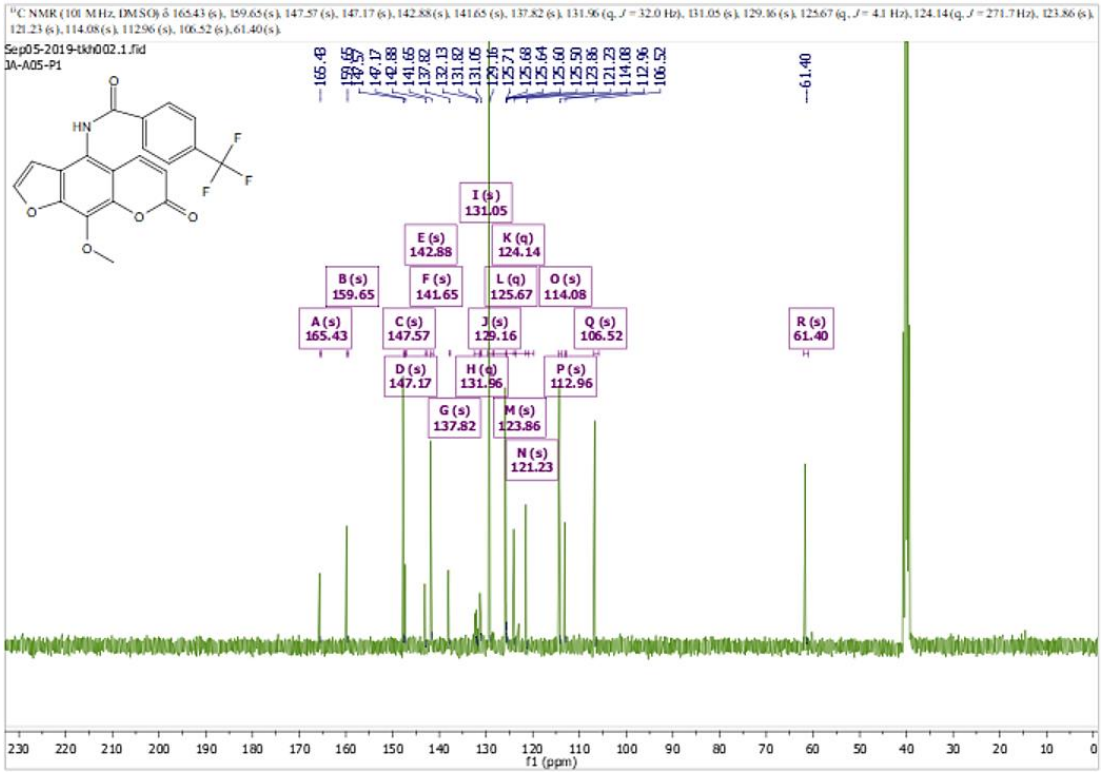

Figure S24 ^{13}C NMR spectrum of **3d**

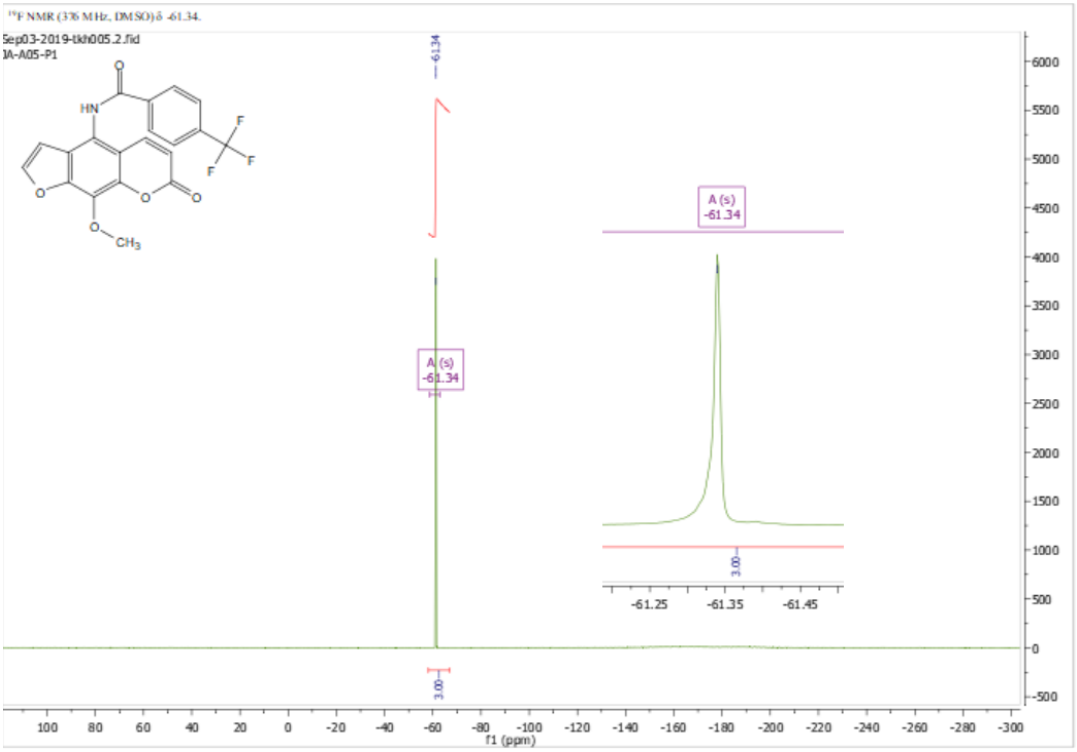

Figure S25 ^{19}F NMR spectrum of **3d**

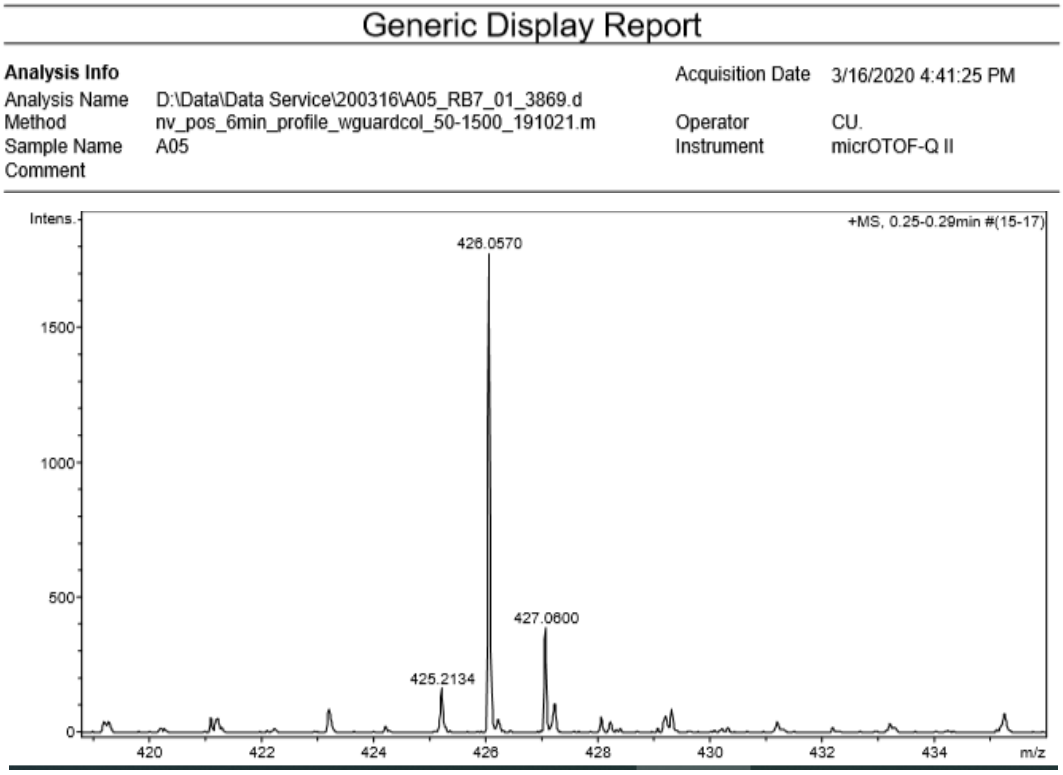

Figure S26 HRMS spectrum of **3d**

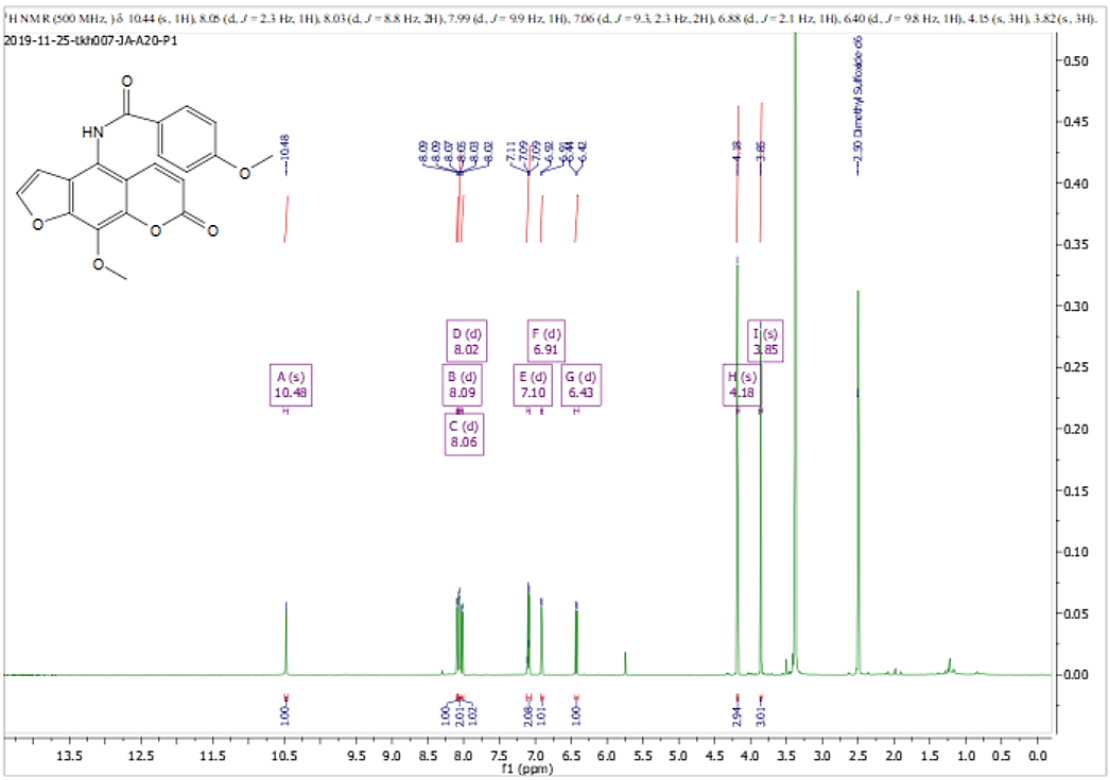

Figure S27 ^{1}H NMR spectrum of **3e**

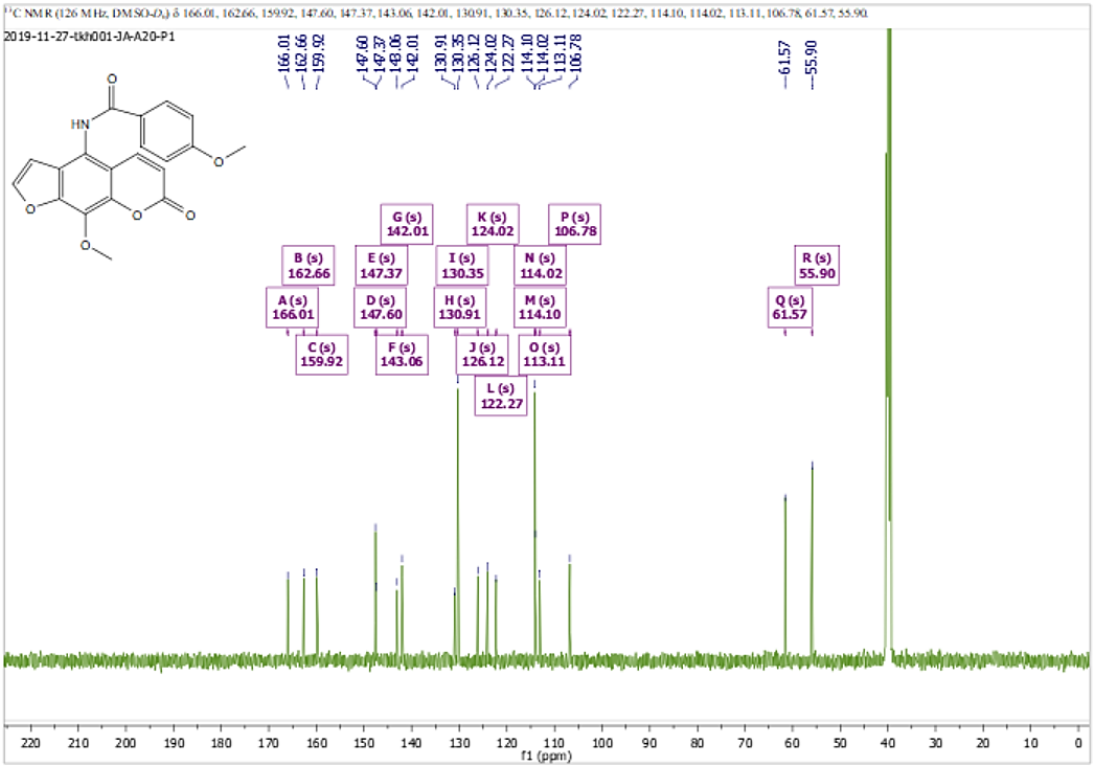

Figure S28 ^{13}C NMR spectrum of **3e**

Generic Display Report

Analysis Info

Analysis Name	D:\Data\Data Service\200316\A20_RC7_01_3877.d	Acquisition Date	3/16/2020 5:35:17 PM
Method	nv_pos_6min_profile_wguardcol_50-1500_191021.m	Operator	CU.
Sample Name	A20	Instrument	micrOTOF-Q II
Comment			

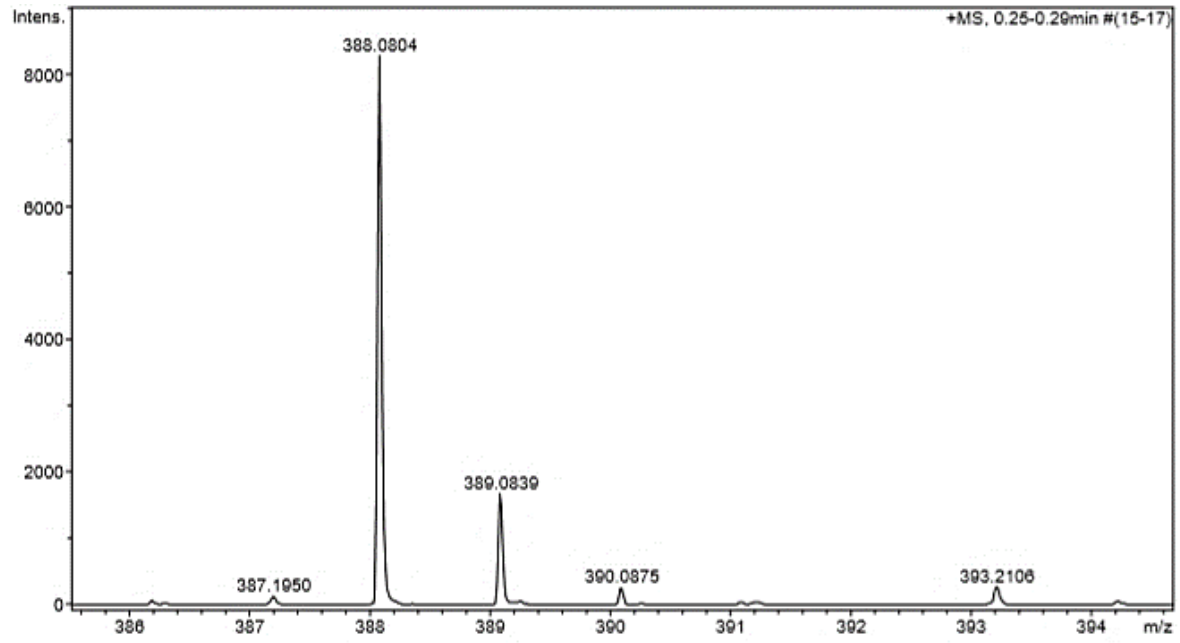

Figure S29 HRMS spectrum of **3e**

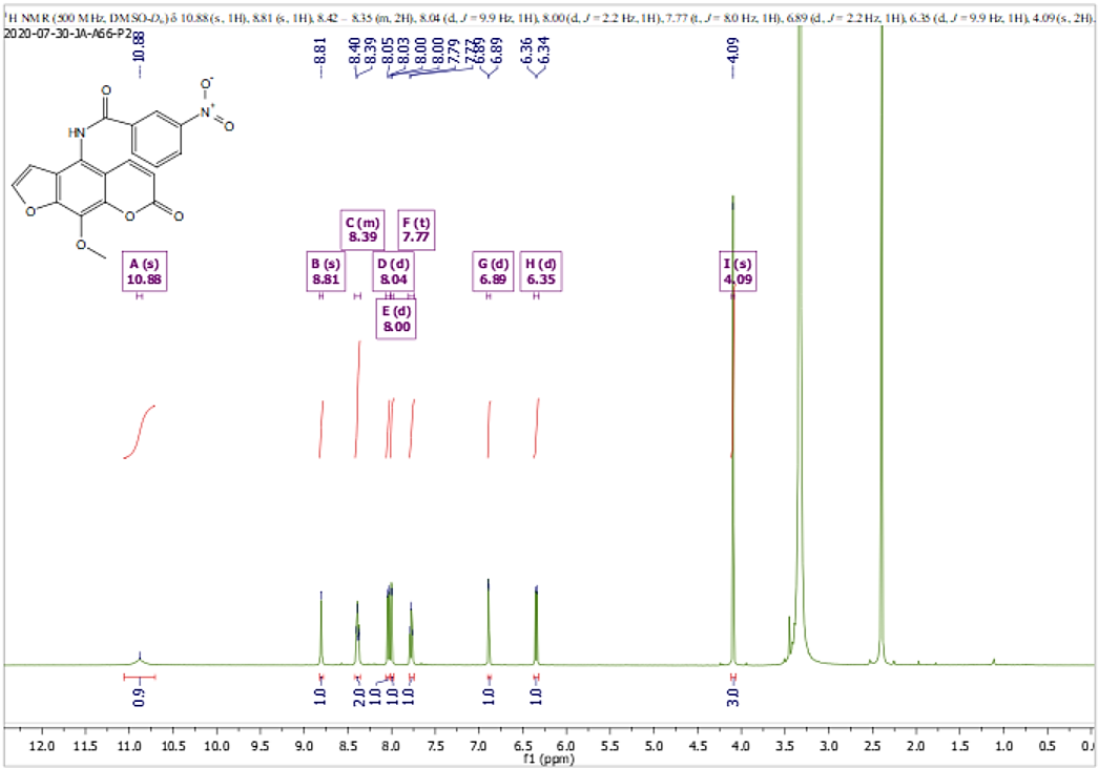

Figure S30 ^{1}H NMR spectrum of **3f**

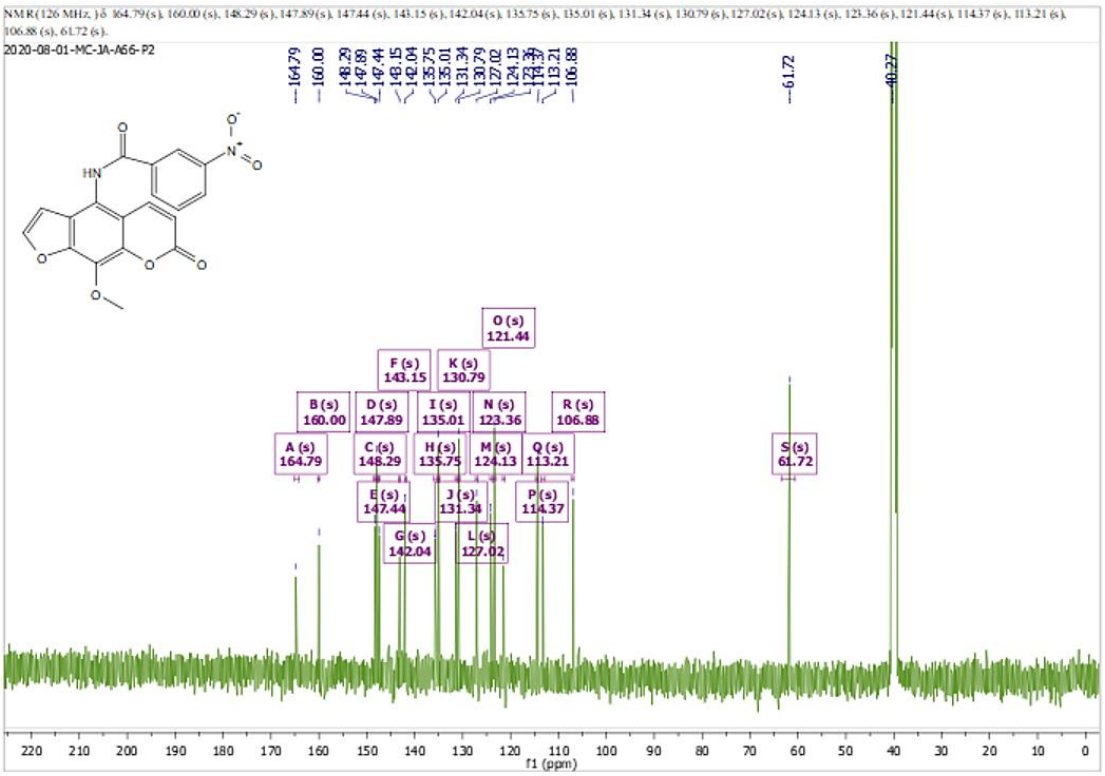

Figure S31 ^{13}C NMR spectrum of **3f**

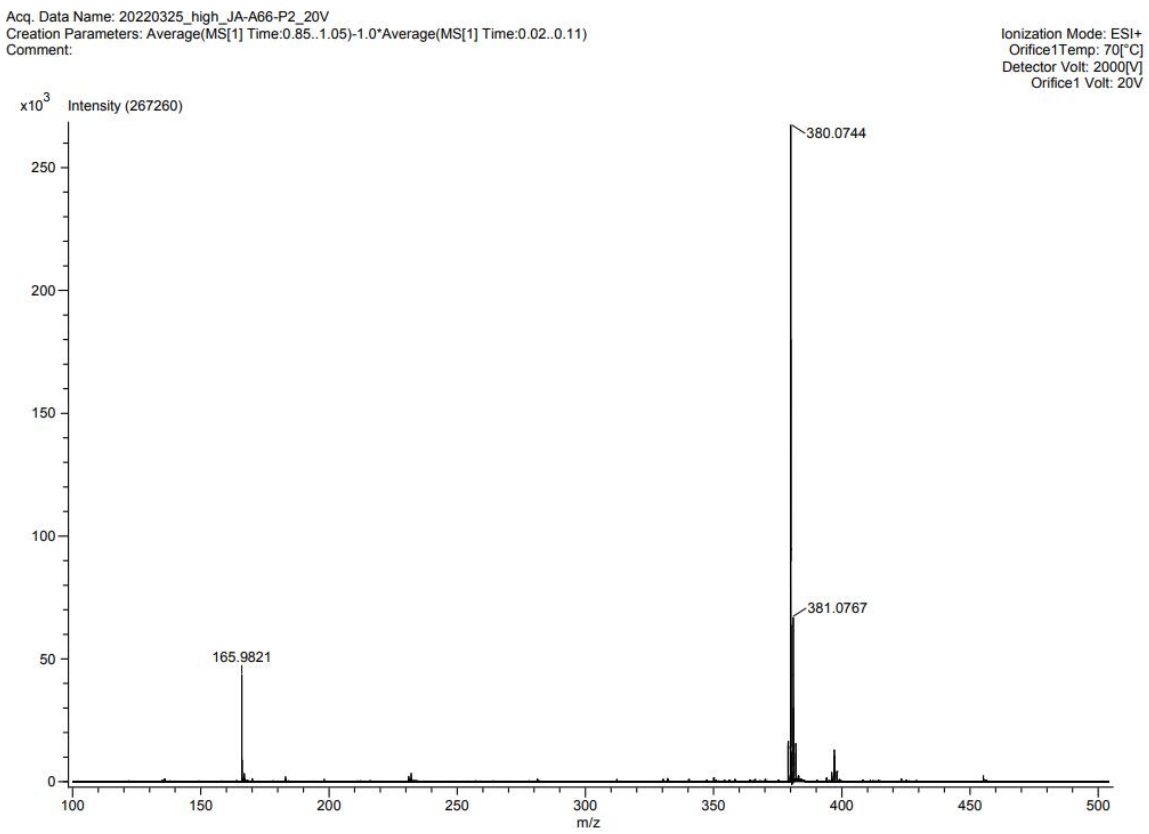

Figure S32 HRMS spectrum of **3f**

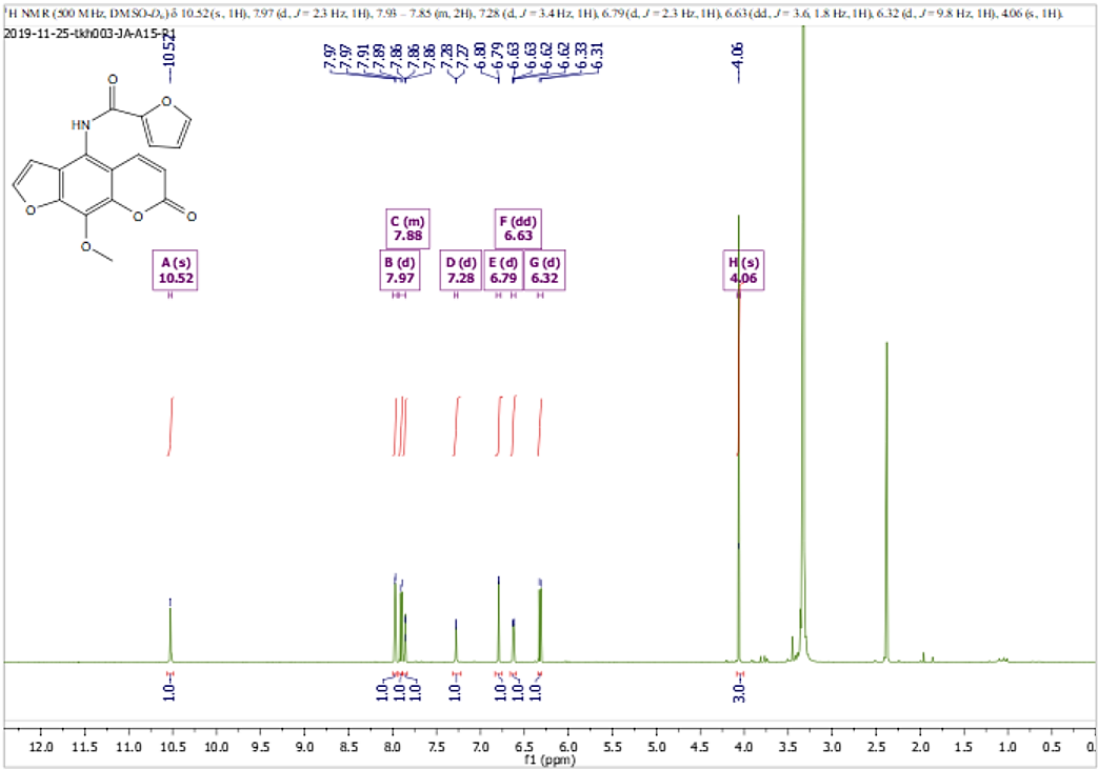

Figure S33 ^{1}H NMR spectrum of **3g**

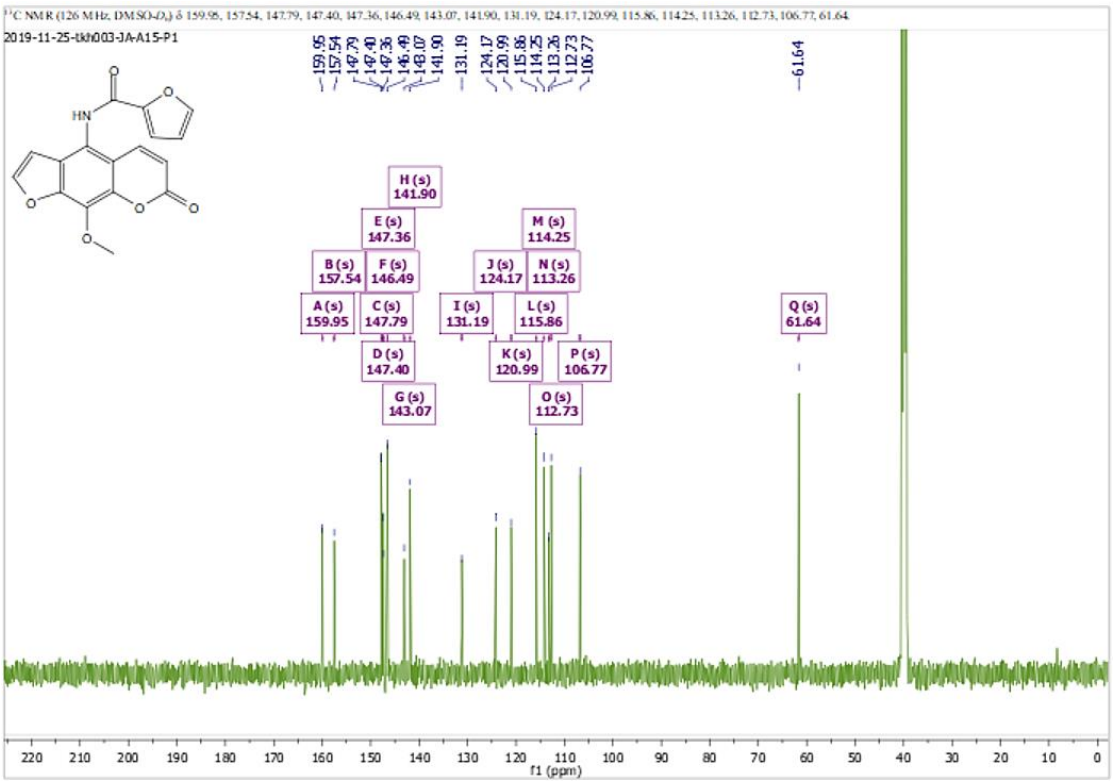

Figure S34 ^{13}C NMR spectrum of **3g**

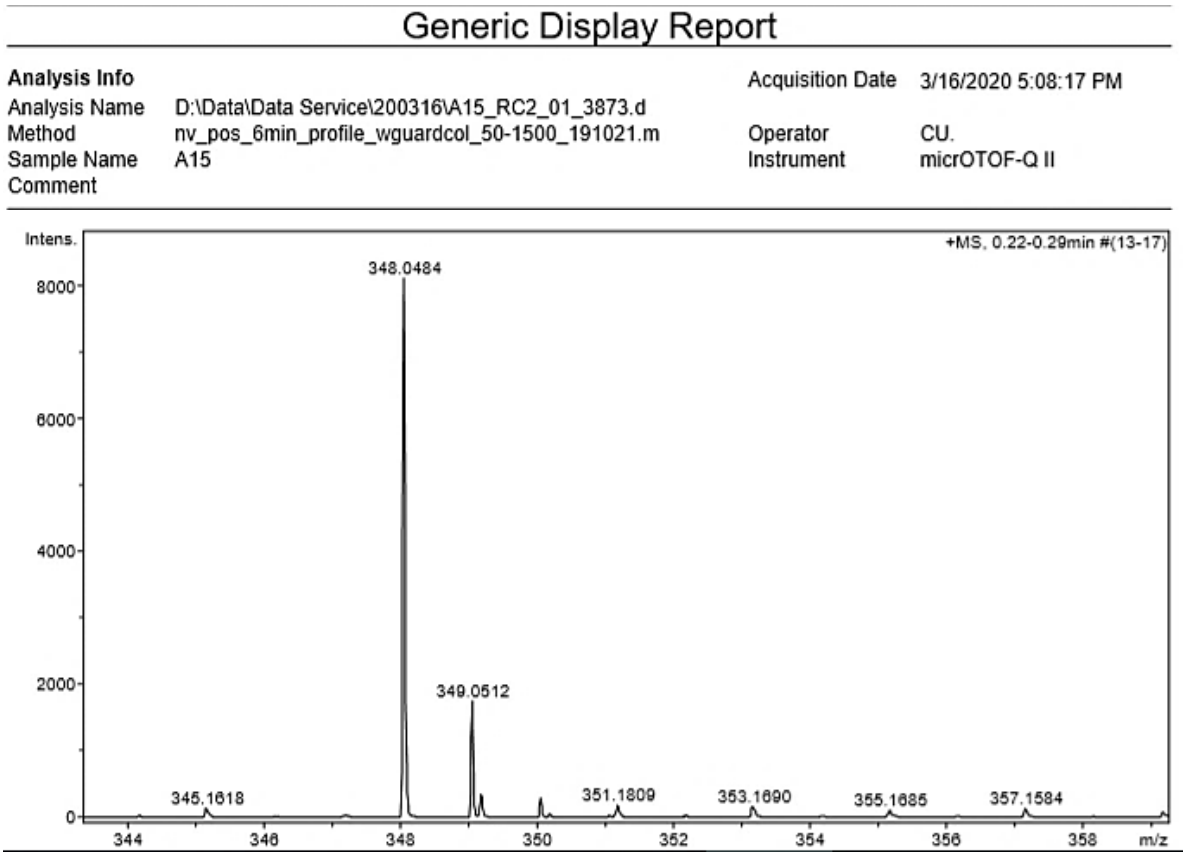

Figure S35 HRMS spectrum of **3g**

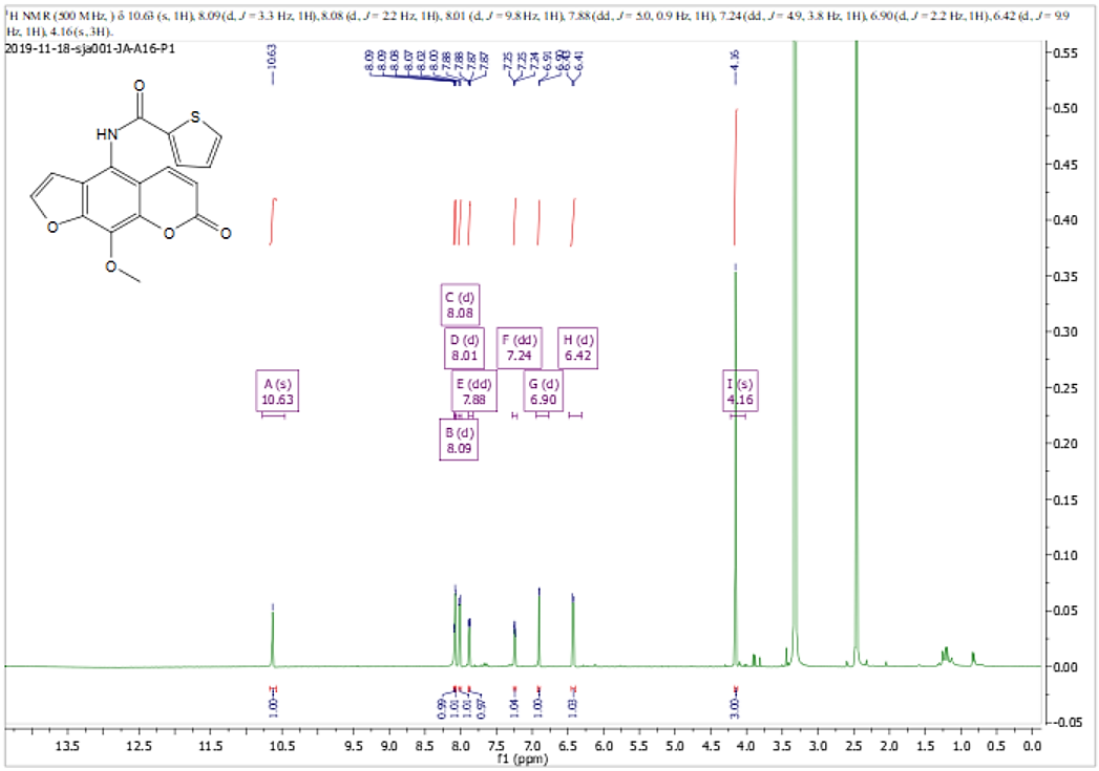

Figure S36 ^{1}H NMR spectrum of **3h**

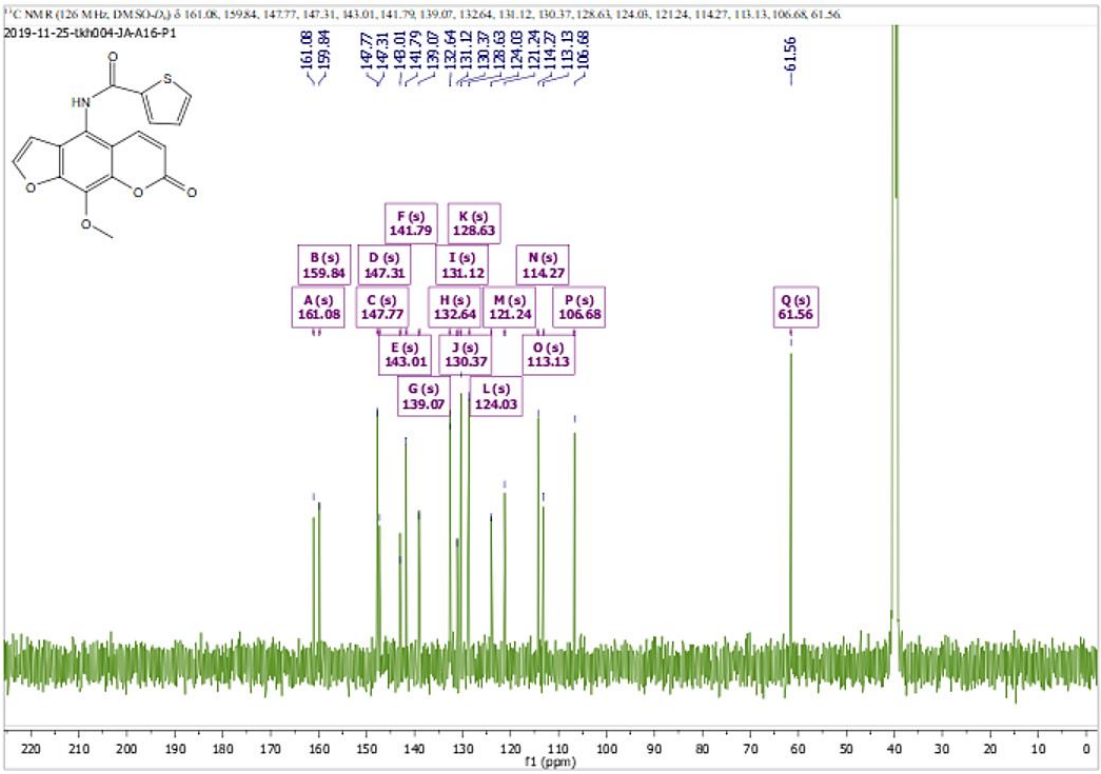

Figure S37 ^{13}C NMR spectrum of **3h**

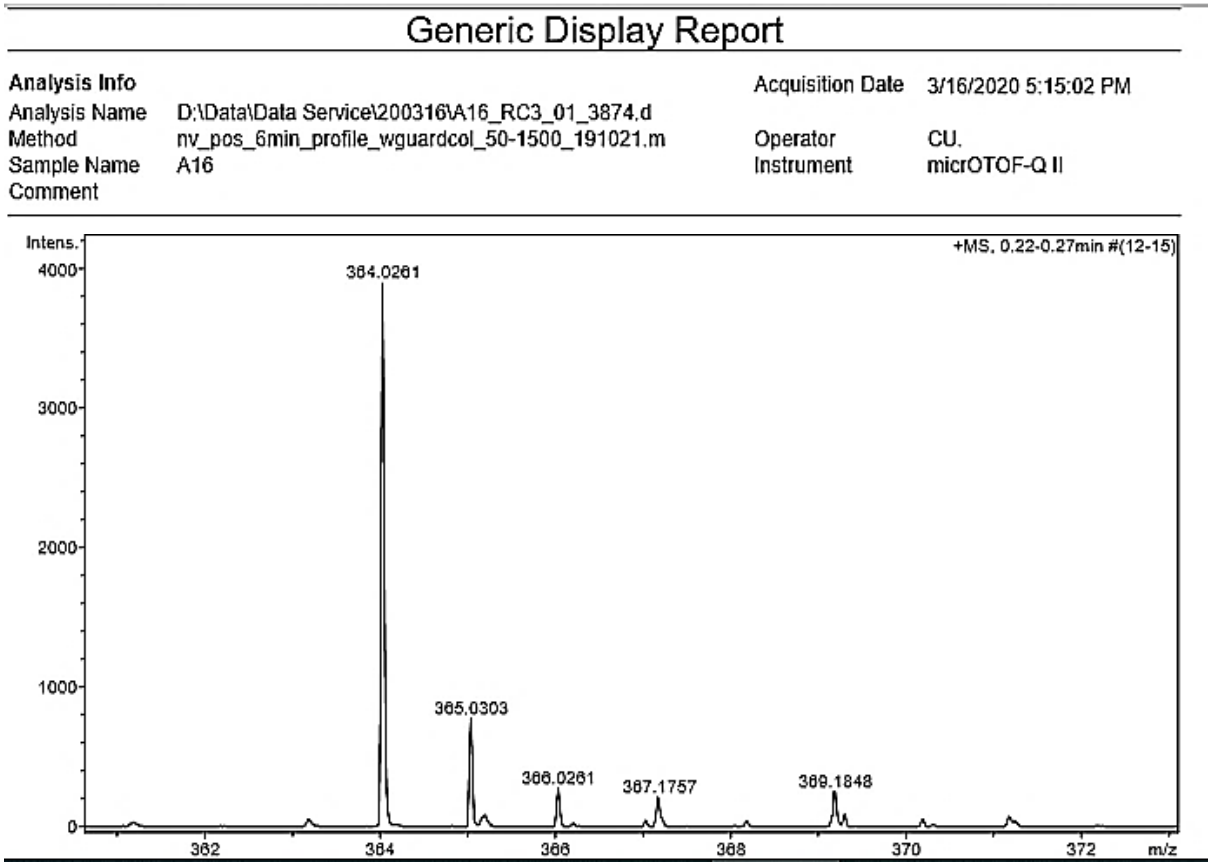

Figure S38 HRMS spectrum of **3h**

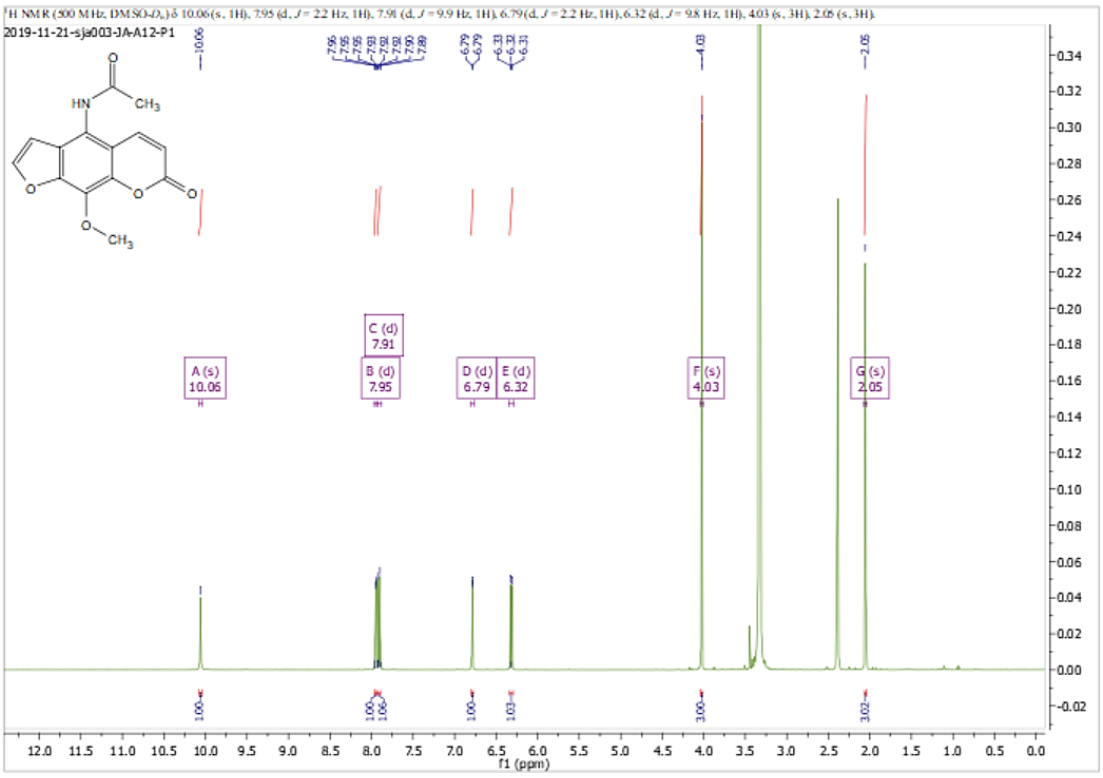

Figure S39 ^{1}H NMR spectrum of **3i**

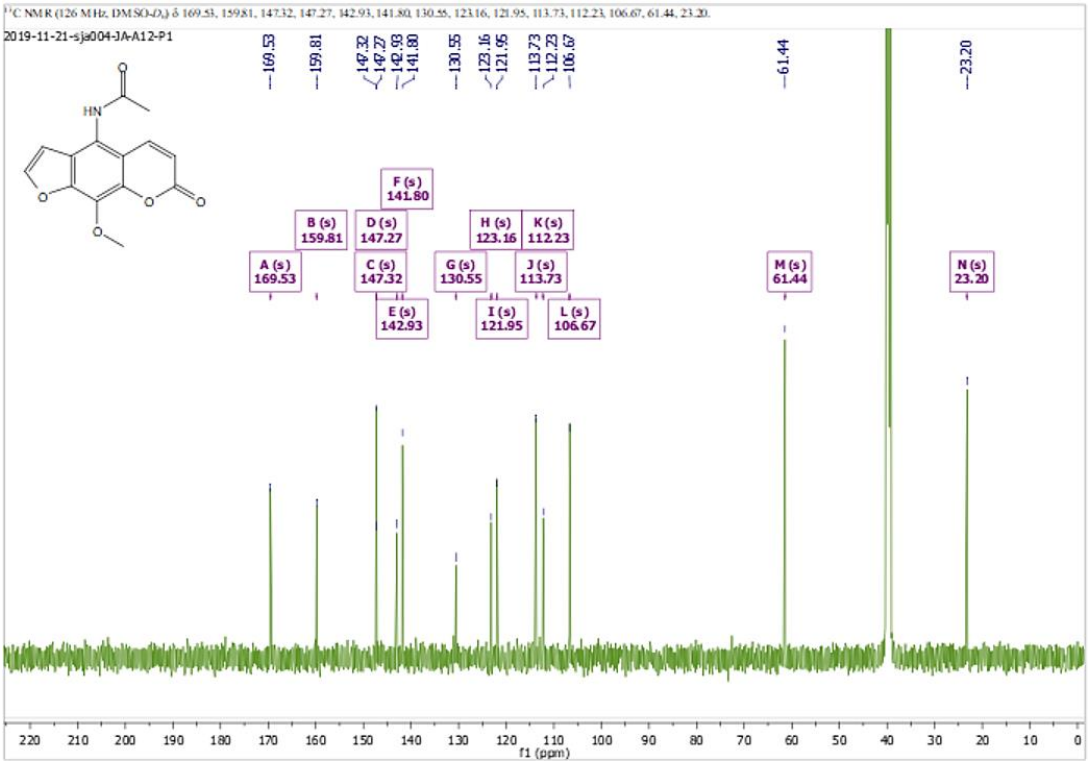

Figure S40 ^{13}C NMR spectrum of **3i**

Generic Display Report

Analysis Info			
Analysis Name	D:\Data\Data Service\200316\A12_RC1_01_3872.d	Acquisition Date	3/16/2020 5:01:31 PM
Method	nv_pos_6min_profile_wguardcol_50-1500_191021.m	Operator	CU.
Sample Name	A12	Instrument	micrOTOF-Q II
Comment			

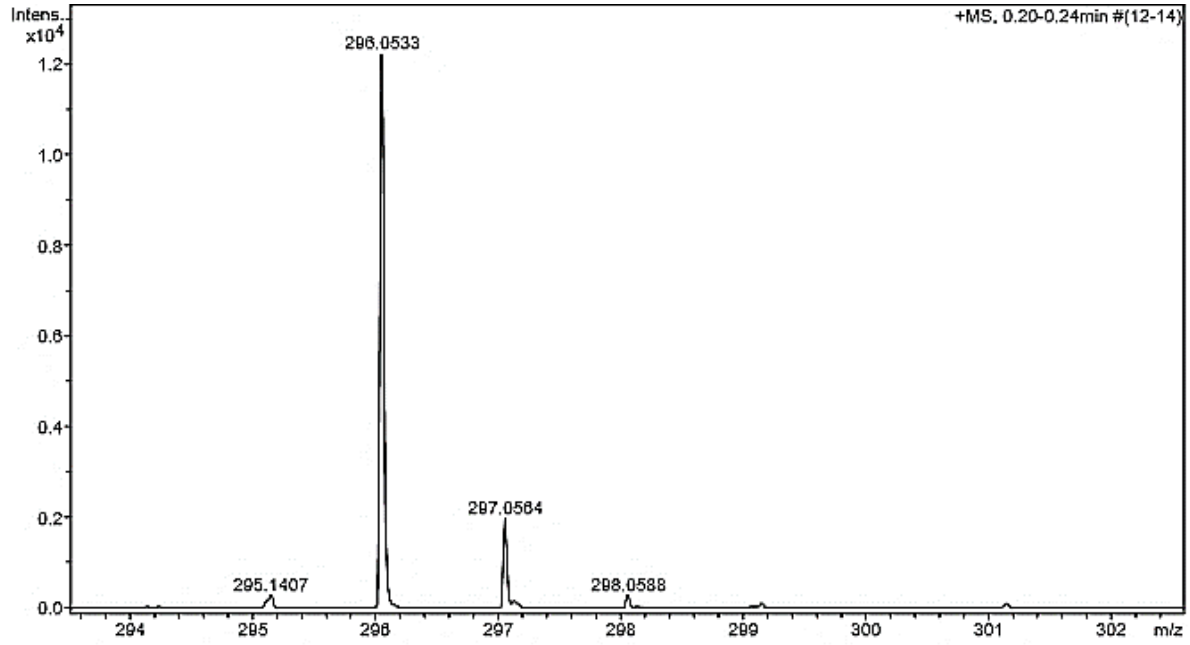

Figure S41 HRMS spectrum of **3i**

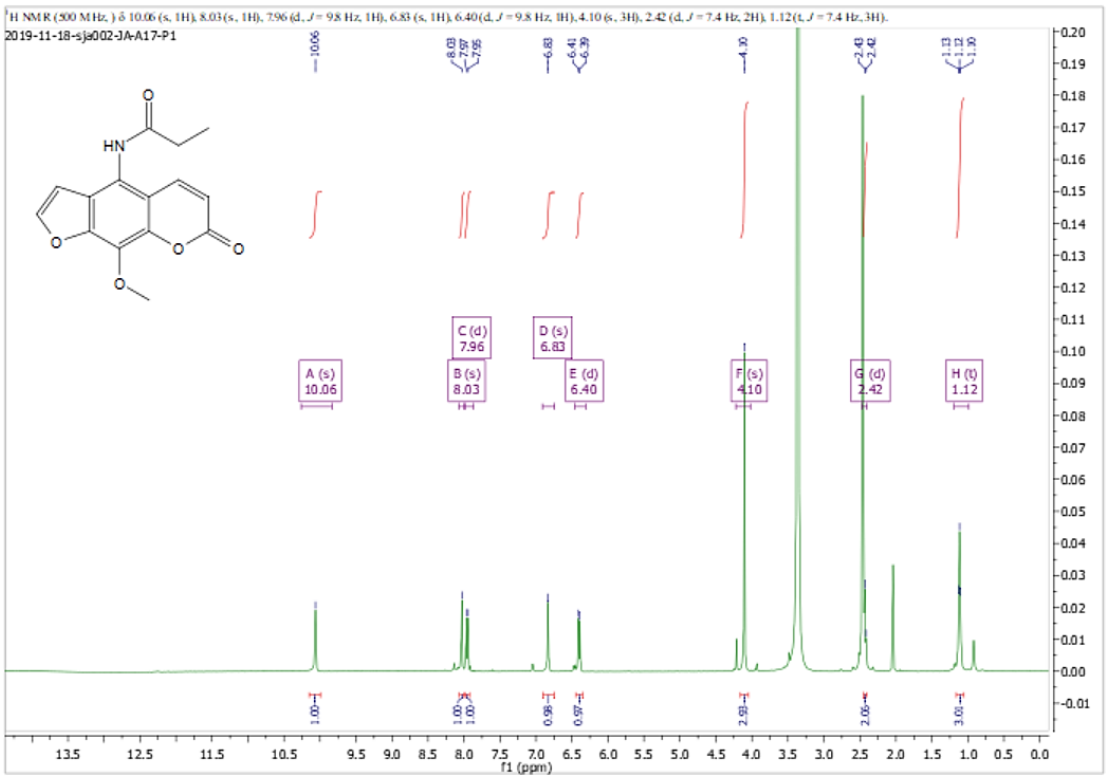

Figure S42 ^{1}H NMR spectrum of **3j**

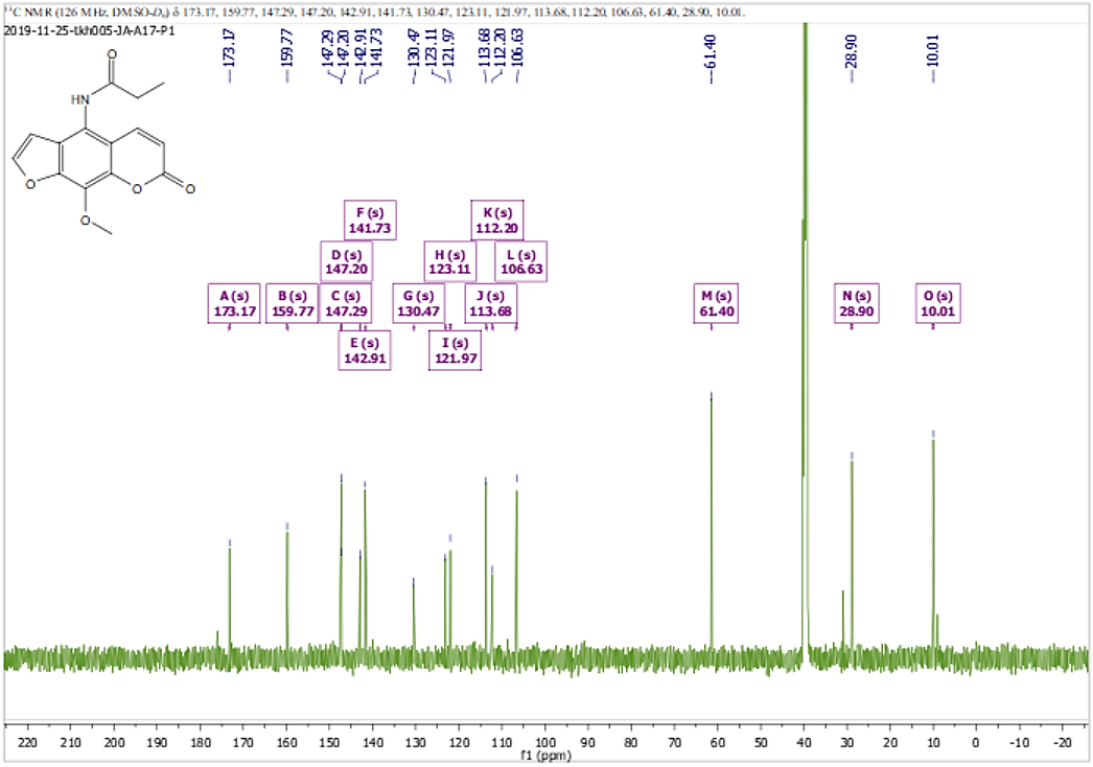

Figure S43 ^{13}C NMR spectrum of **3j**

Generic Display Report

Analysis Info			
Analysis Name	D:\Data\Data Service\200316\A17_RC4_01_3875.d	Acquisition Date	3/16/2020 5:21:46 PM
Method	nv_pos_6min_profile_wguardcol_50-1500_191021.m	Operator	CU.
Sample Name	A17	Instrument	micrOTOF-Q II
Comment			

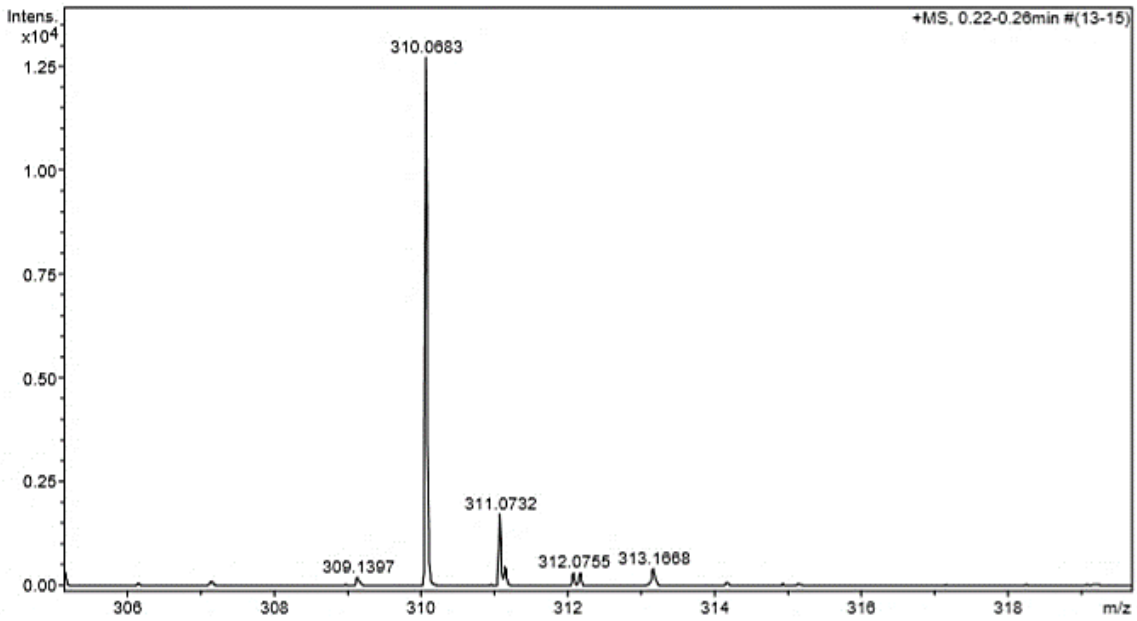

Figure S44 HRMS spectrum of **3j**

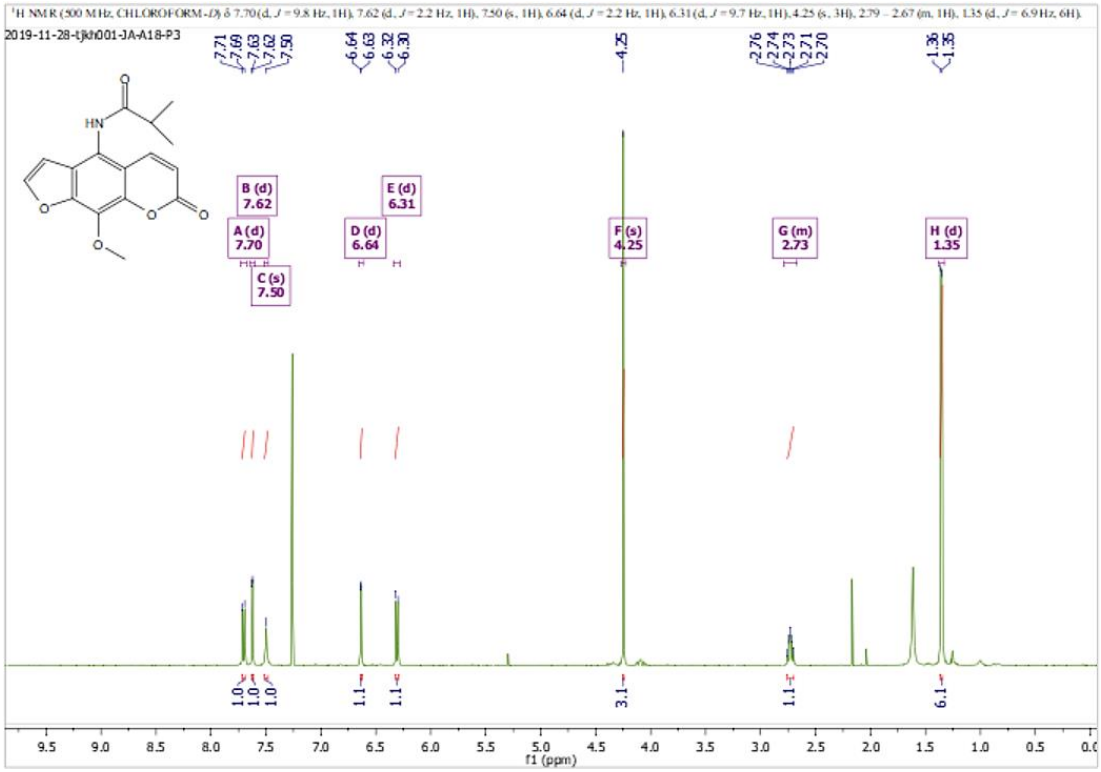

Figure S45 ^{1}H NMR spectrum of **3k**

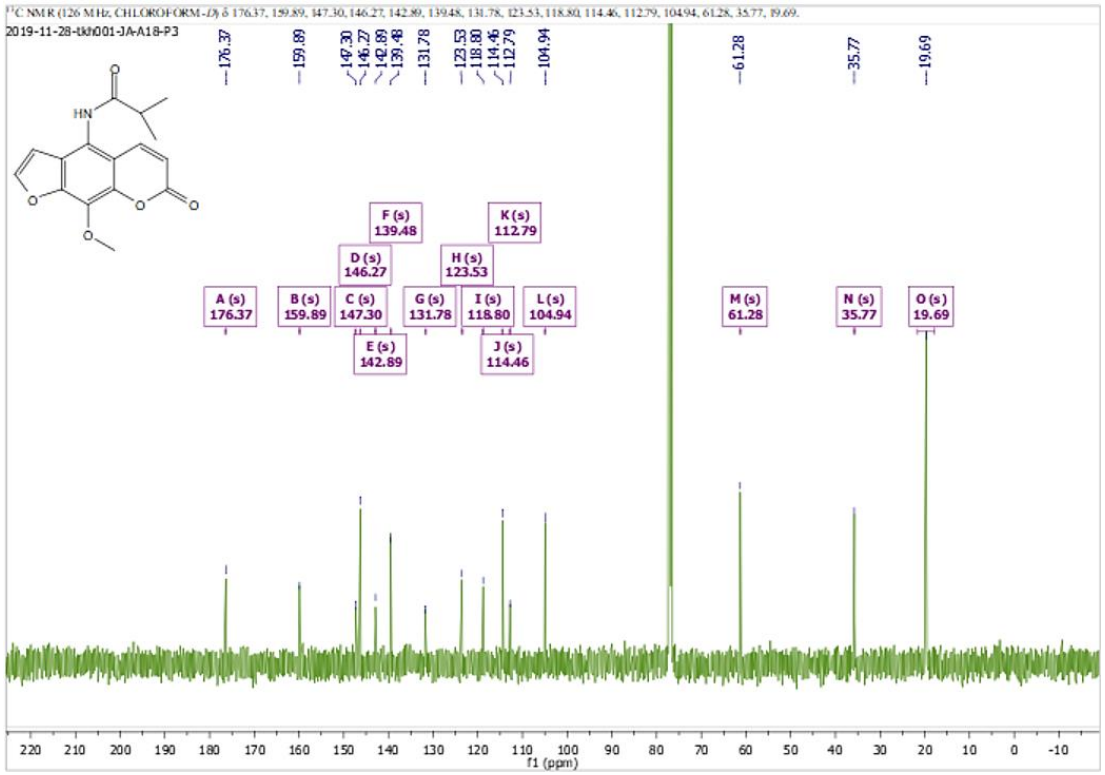

Figure S46 ^{13}C NMR spectrum of **3k**

Generic Display Report

Analysis Info

Analysis Name	D:\Data\Data Service\200316\A18_RC5_01_3861.d	Acquisition Date	3/16/2020 3:37:32 PM
Method	nv_pos_6min_profile_wguardcol_50-1500_191021.m	Operator	CU.
Sample Name	A18	Instrument	micrOTOF-Q II
Comment			

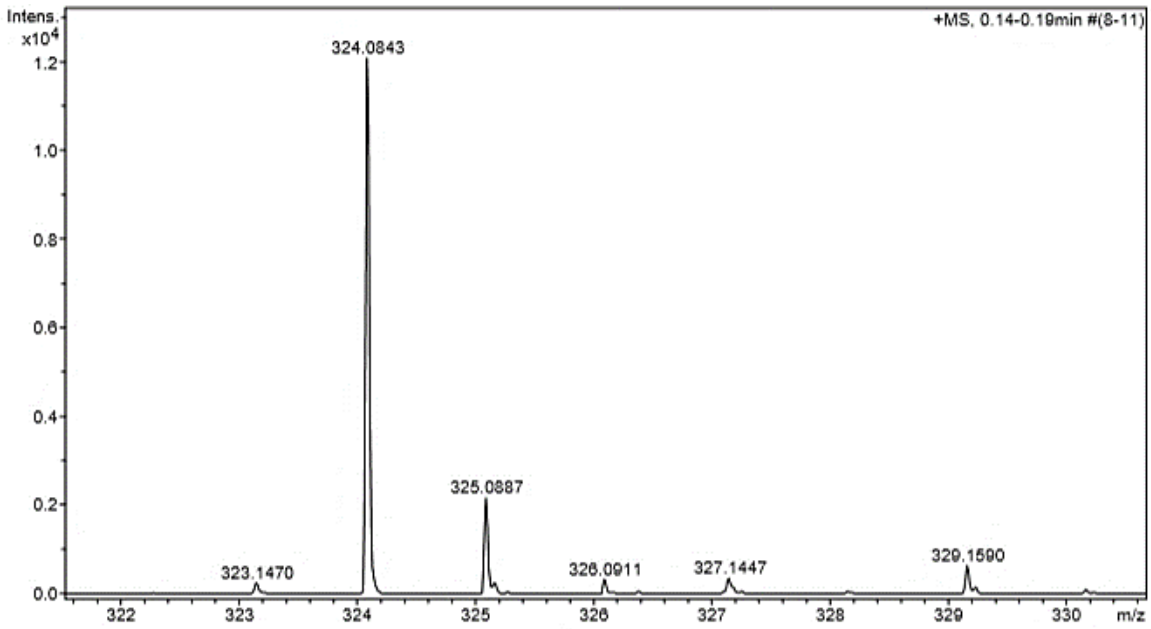

Figure S47 HRMS spectrum of **3k**

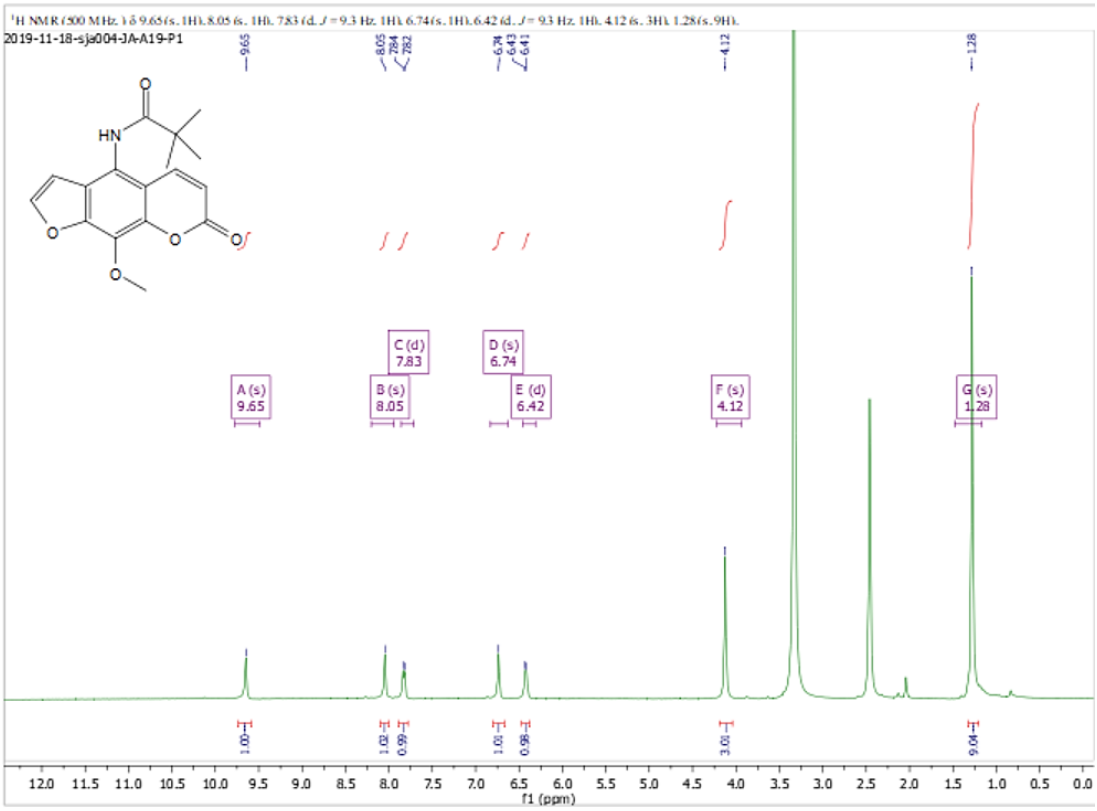

Figure S48 ^{1}H NMR spectrum of **3l**

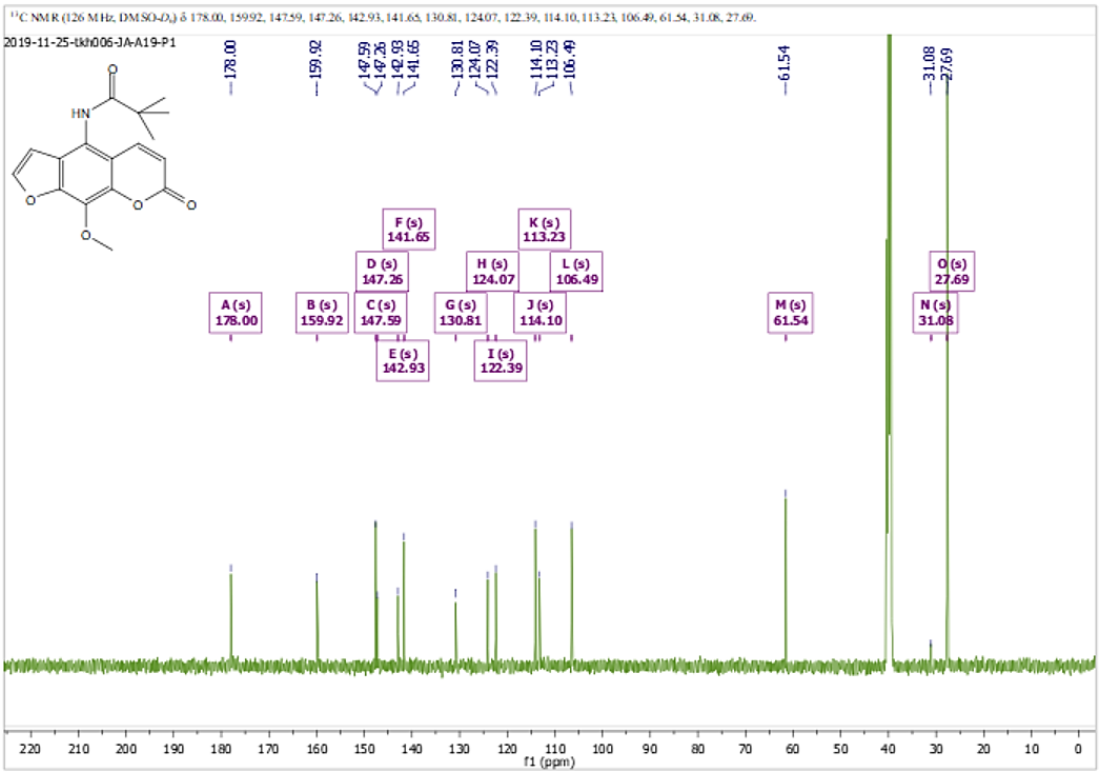

Figure S49 ^{13}C NMR spectrum of **3l**

Generic Display Report

Analysis Info

Analysis Name	D:\Data\Data Service\200316\A19_RC6_01_3876.d	Acquisition Date	3/16/2020 5:28:30 PM
Method	nv_pos_6min_profile_wguardcol_50-1500_191021.m	Operator	CU.
Sample Name	A19	Instrument	micrOTOF-Q II
Comment			

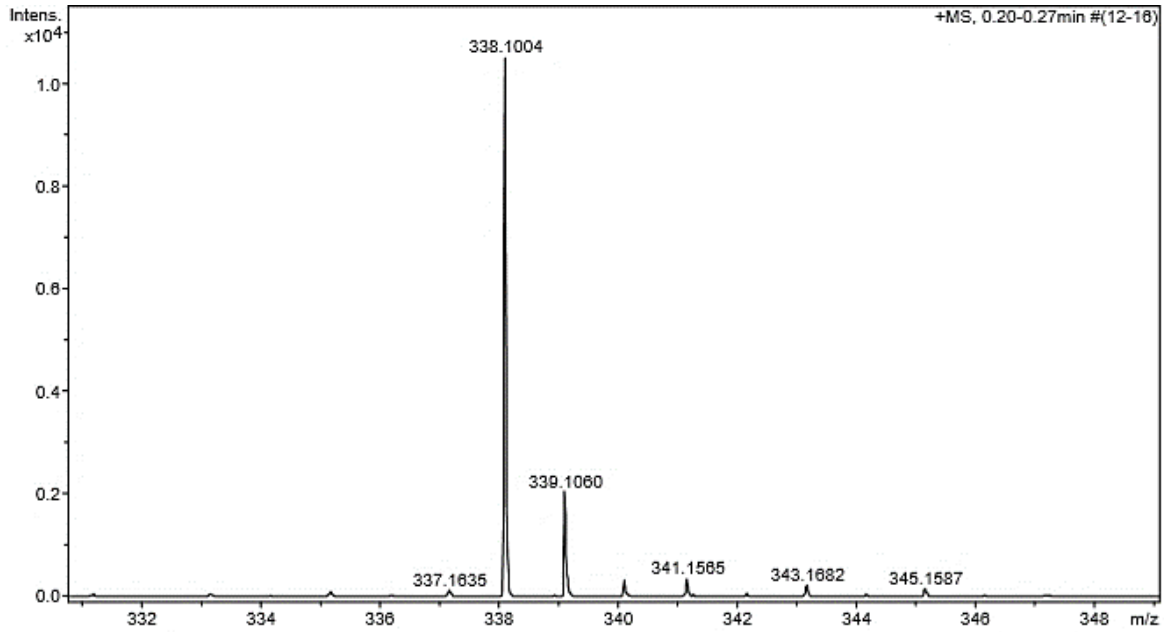

Figure S50 HRMS spectrum of **3l**

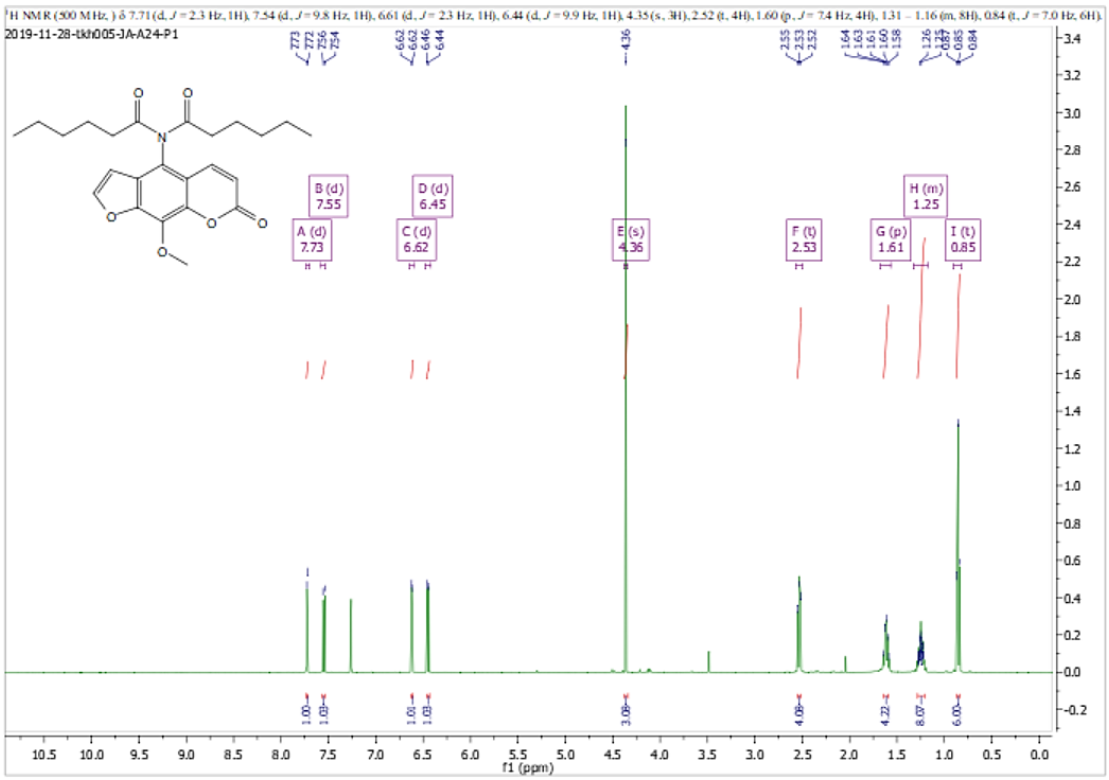

Figure S51 ^{1}H NMR spectrum of **3m**

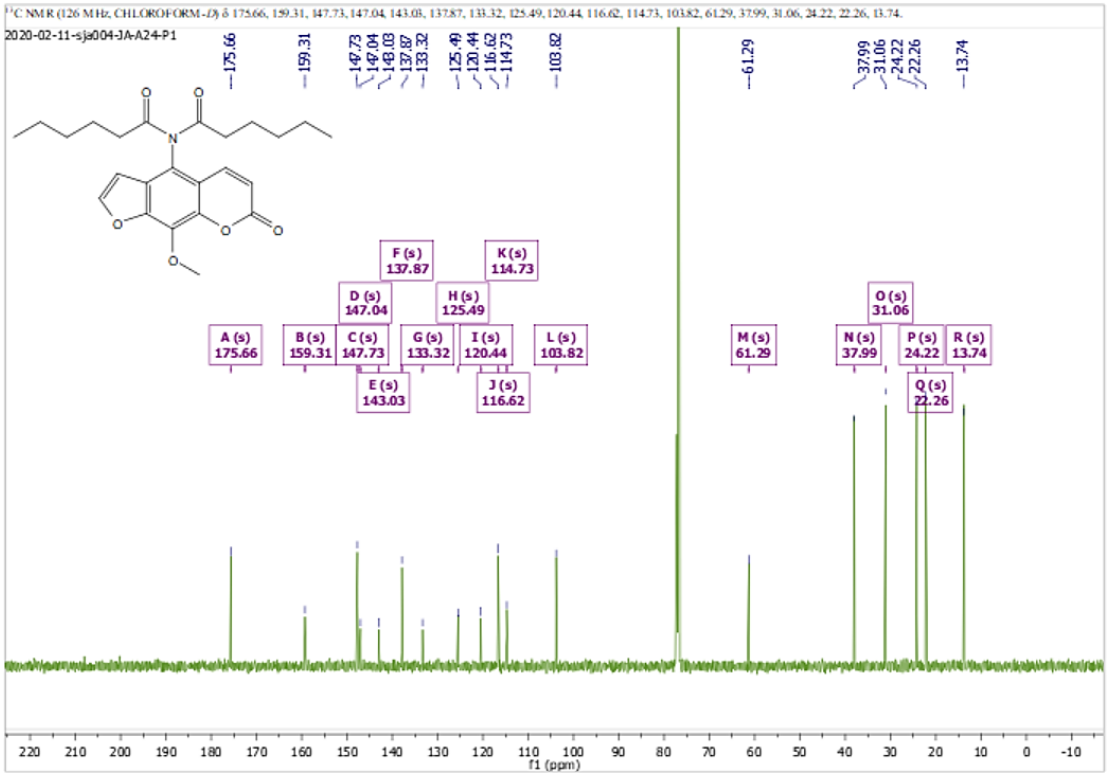

Figure S52 ^{13}C NMR spectrum of **3m**

Generic Display Report

Analysis Info

Analysis Name	D:\Data\Data Service\200316\A24_RC8_01_3878.d	Acquisition Date	3/16/2020 5:42:02 PM
Method	nv_pos_6min_profile_wguardcol_50-1500_191021.m	Operator	CU.
Sample Name	A24	Instrument	micrOTOF-Q II
Comment			

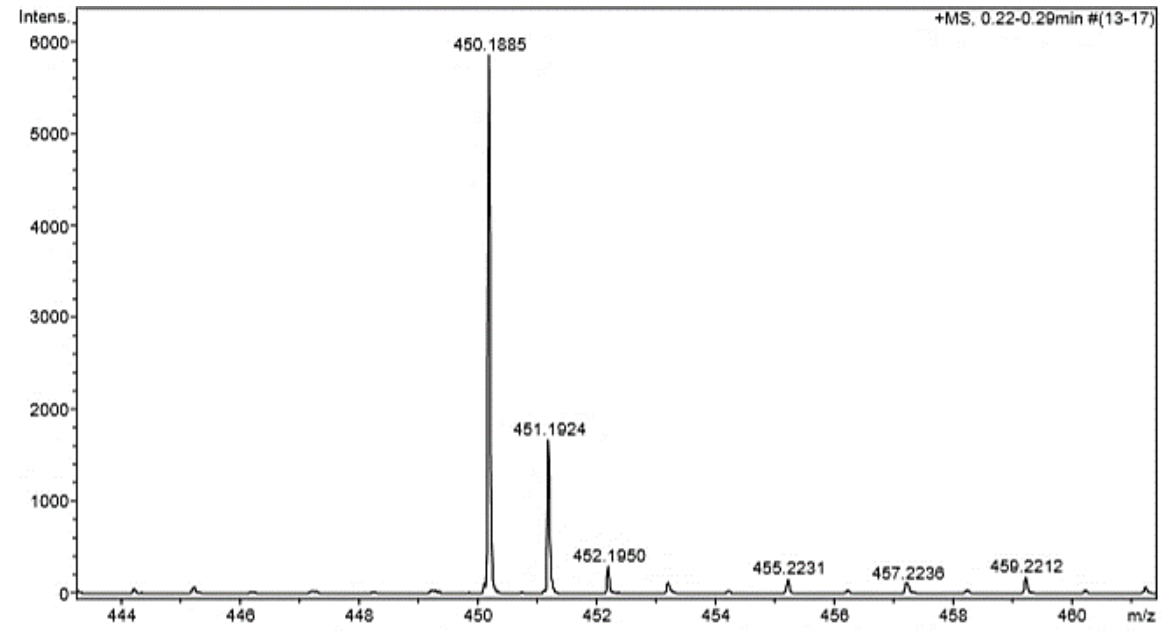

Figure S53 HRMS spectrum of **3m**

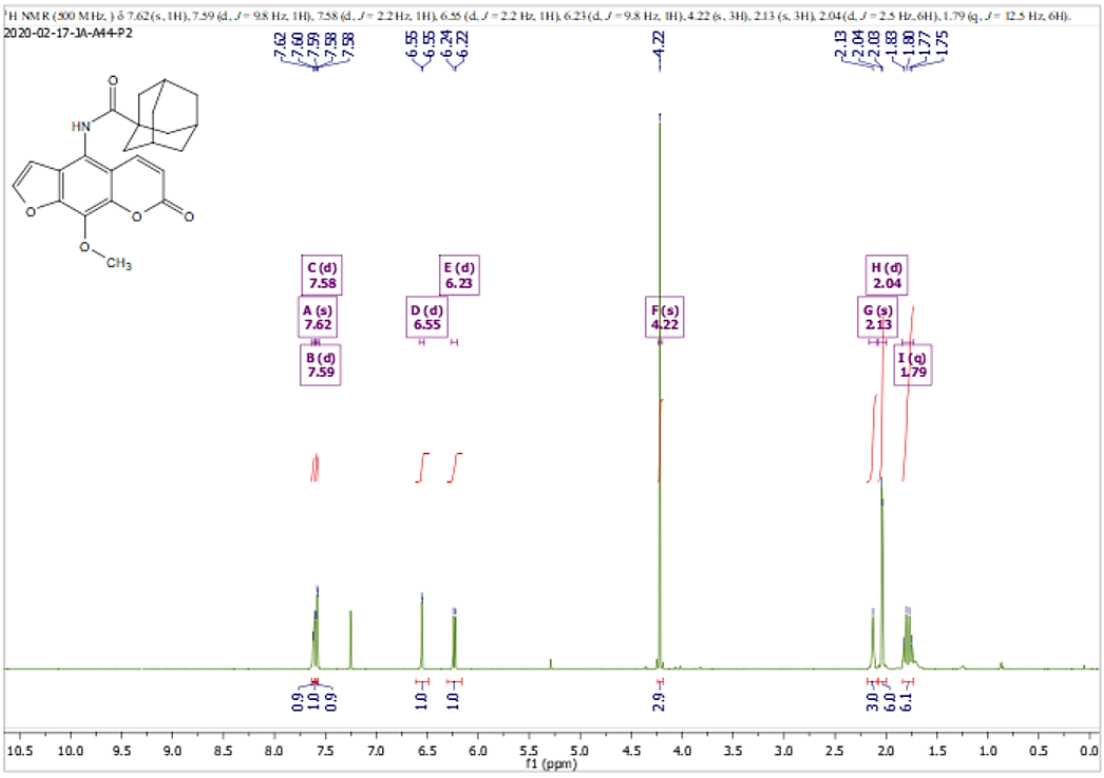

Figure S54 ^{1}H NMR spectrum of **3n**

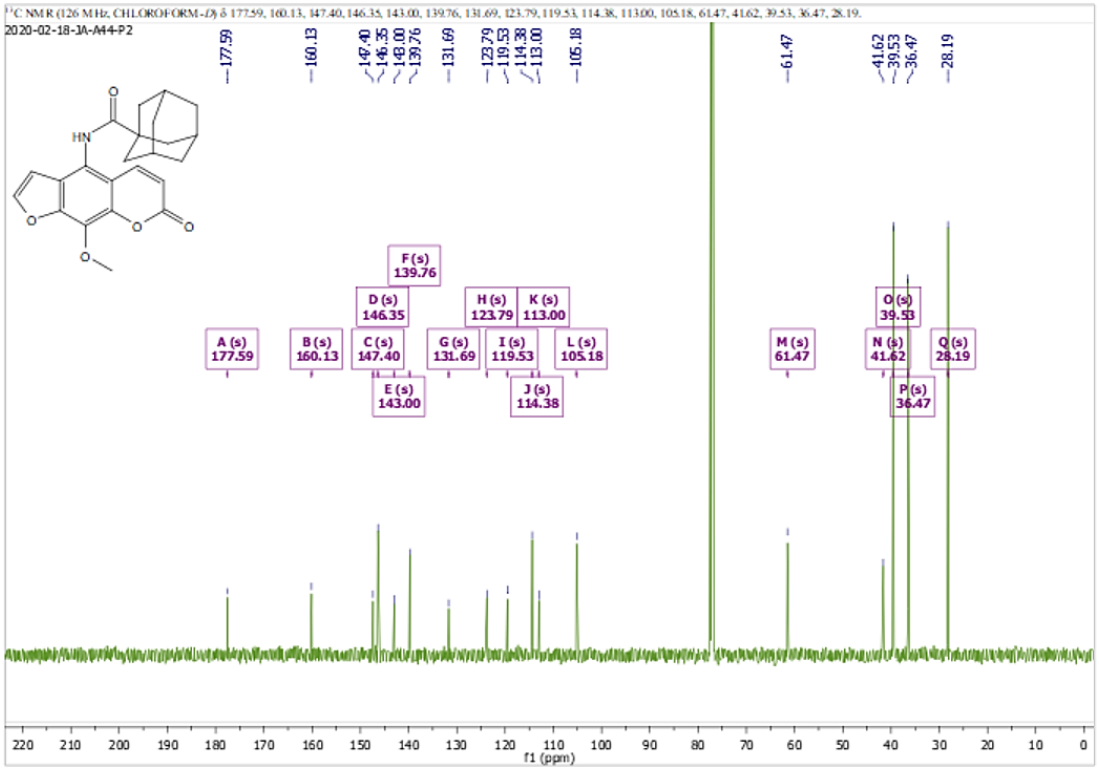

Figure S55 ^{13}C NMR spectrum of **3n**

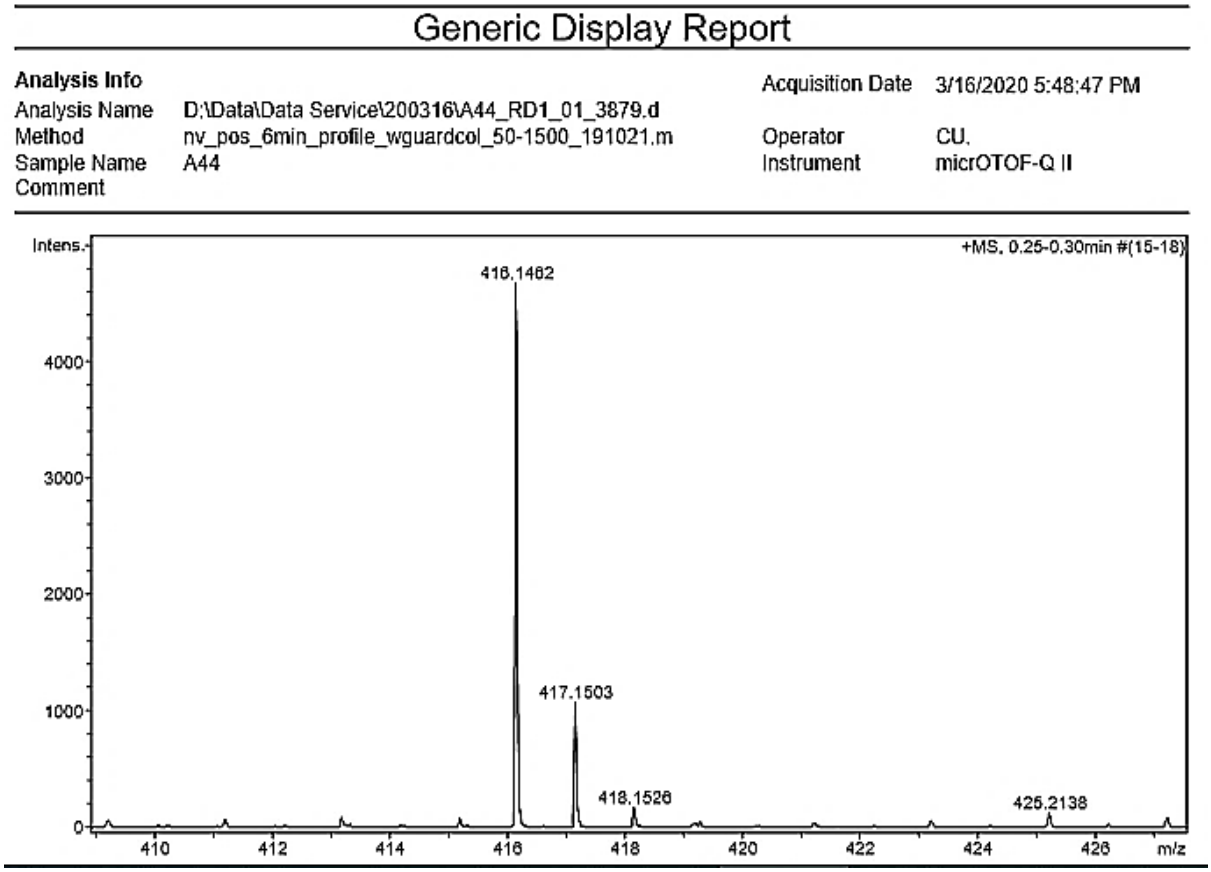

Figure S56 HRMS spectrum of **3n**

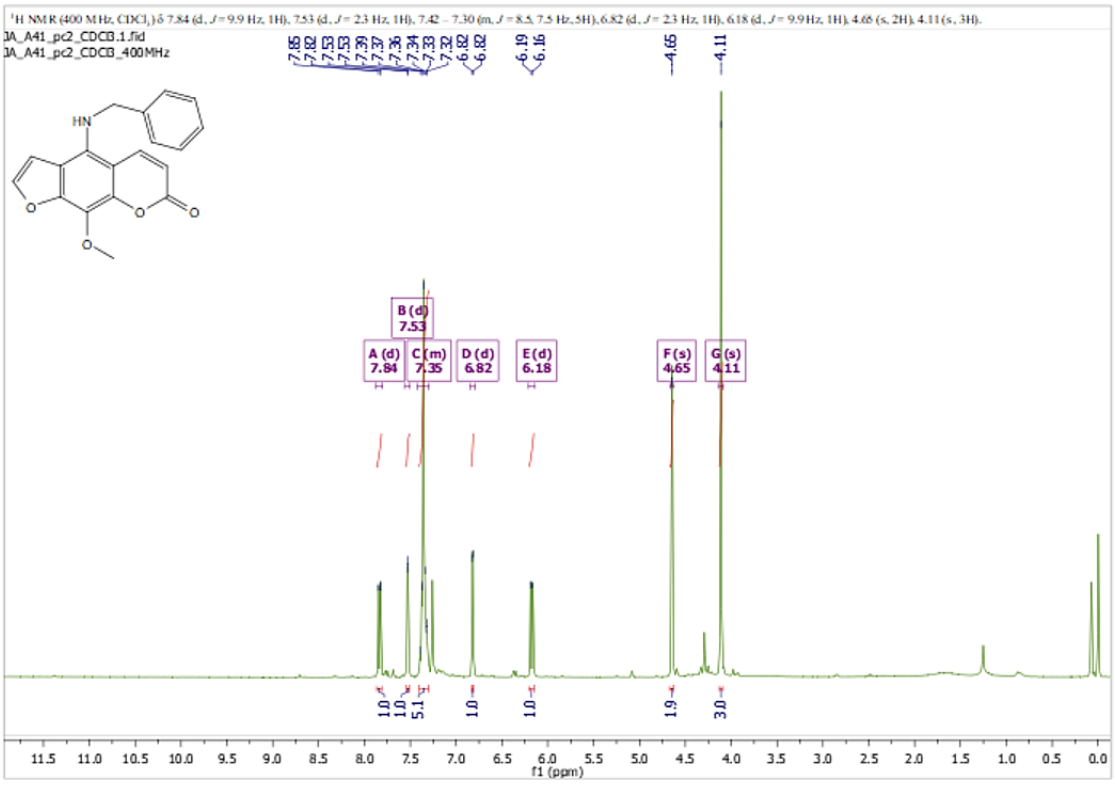

Figure S57 ^{1}H NMR spectrum of **4a**

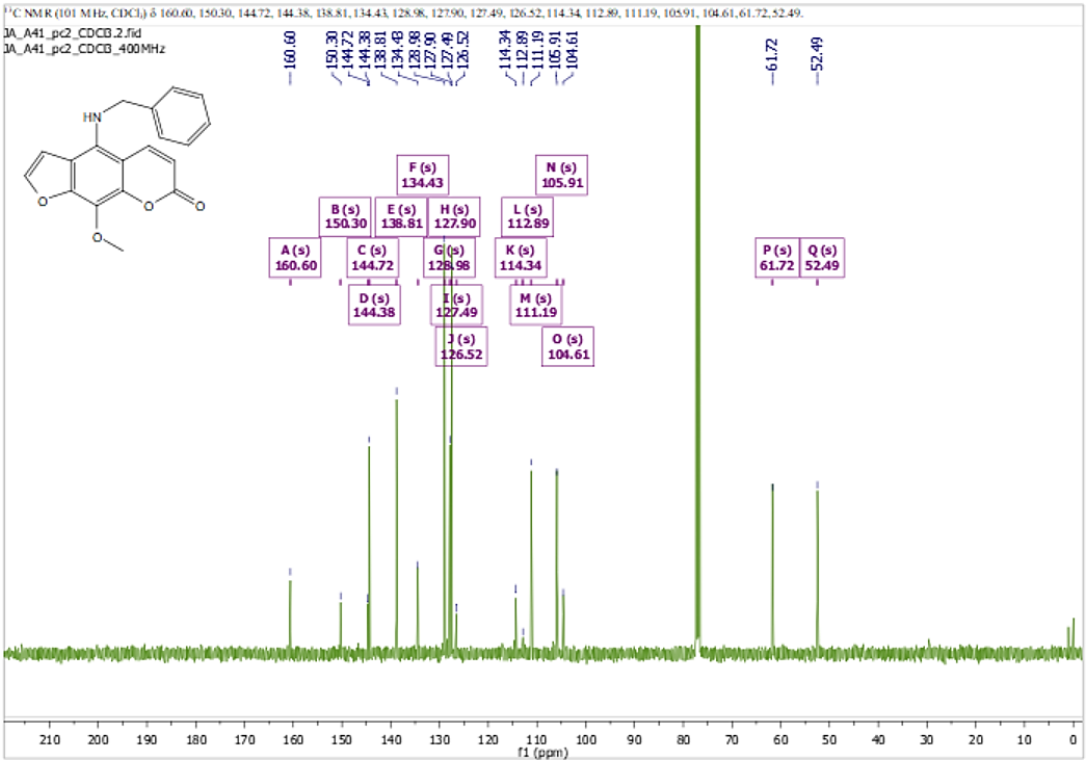

Figure S58 ^{13}C NMR spectrum of **4a**

Mass Spectrum List Report

Analysis Info

Analysis Name	TOFCRI25780 Jutatip JA741-PC2 E+.d	Acquisition Date	12/27/2019 1:54:37 AM
Method	Nitirat ESI pos 2019-1.m	Operator	Administrator
Sample Name	ESIpos	Instrument	micrOTOF 74

Acquisition Parameter

Source Type	ESI	Ion Polarity	Positive	Set Corrector Fill	64 V
Scan Range	n/a	Capillary Exit	110.0 V	Set Pulsar Pull	405 V
Scan Begin	100 m/z	Hexapole RF	160.0 V	Set Pulsar Push	405 V
Scan End	850 m/z	Skimmer 1	33.0 V	Set Reflector	1300 V
		Hexapole 1	22.9 V	Set Flight Tube	9000 V
				Set Detector TOF	1988 V

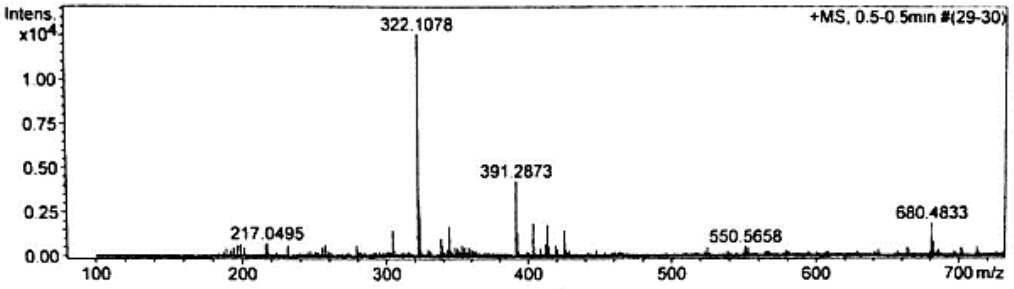

Figure S59 HRMS spectrum of **4a**

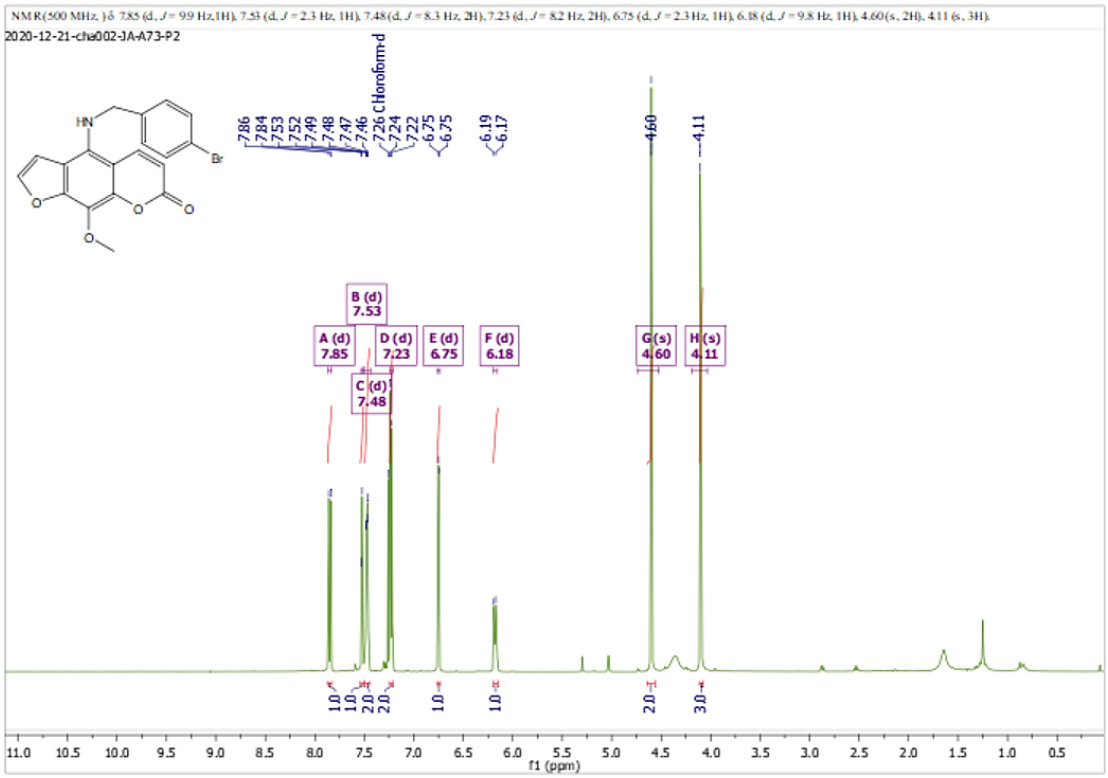

Figure S60 ^{1}H NMR spectrum of **4b**

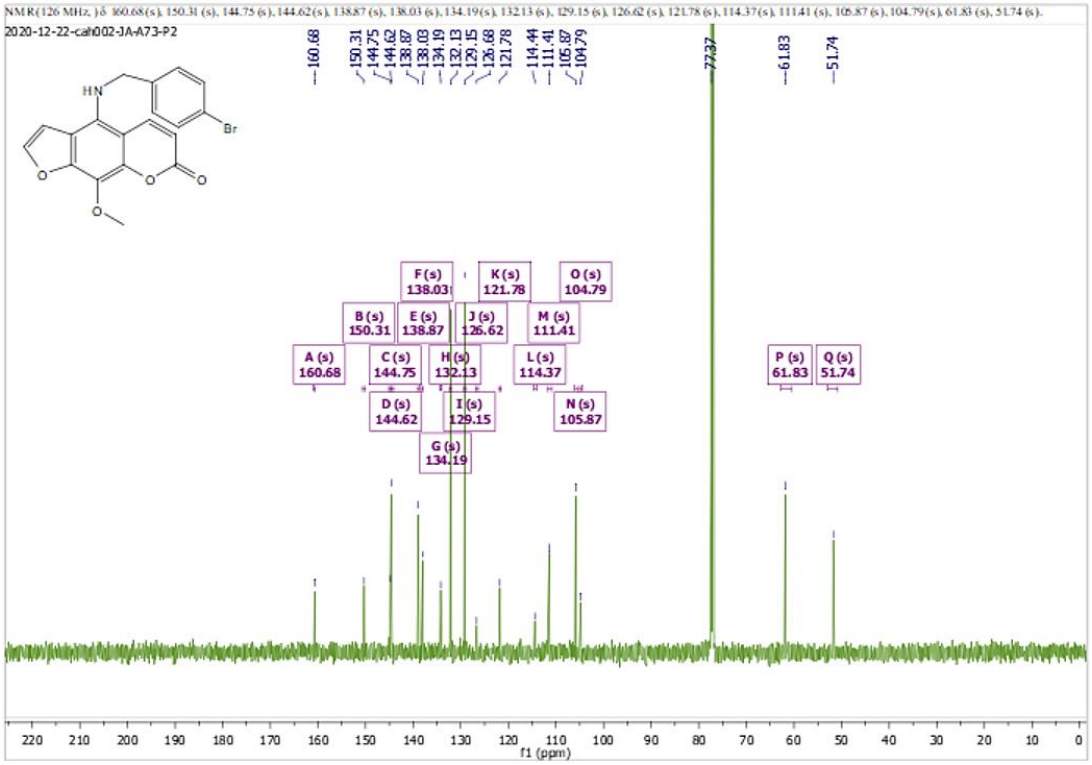

Figure S61 ^{13}C NMR spectrum of **4b**

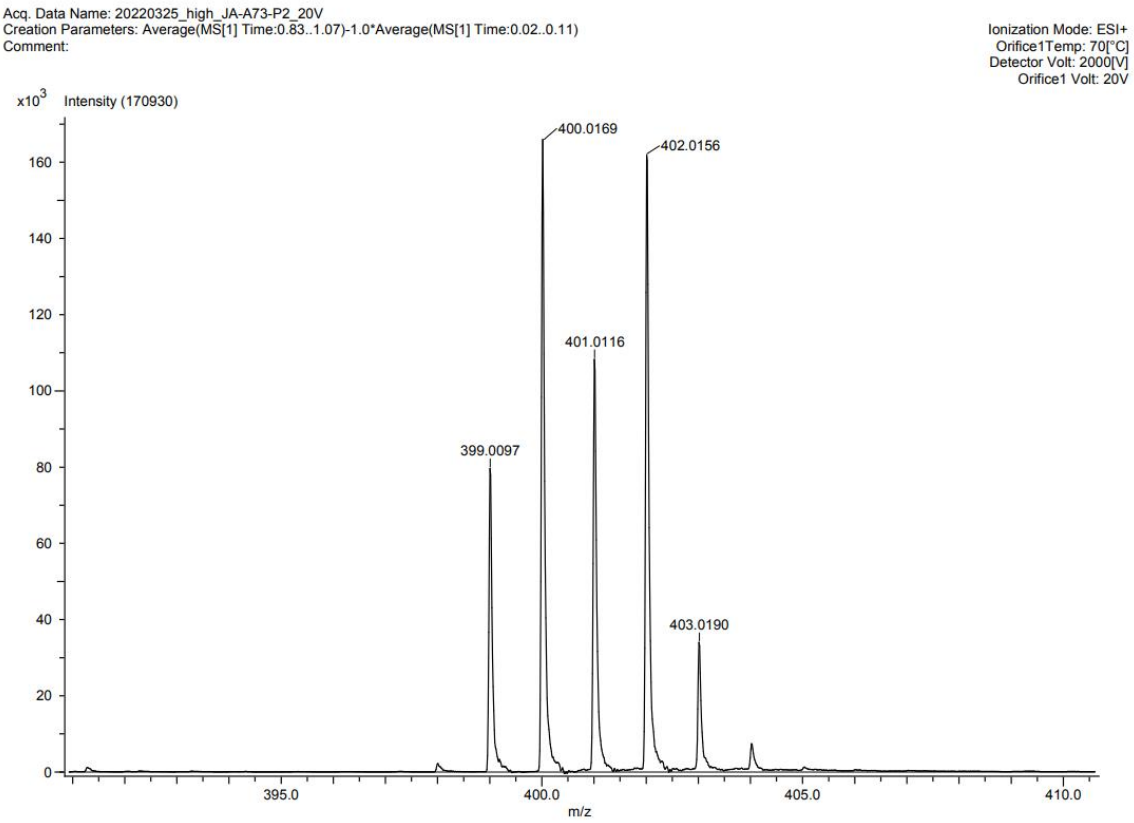

Figure S62 HRMS spectrum of **4b**

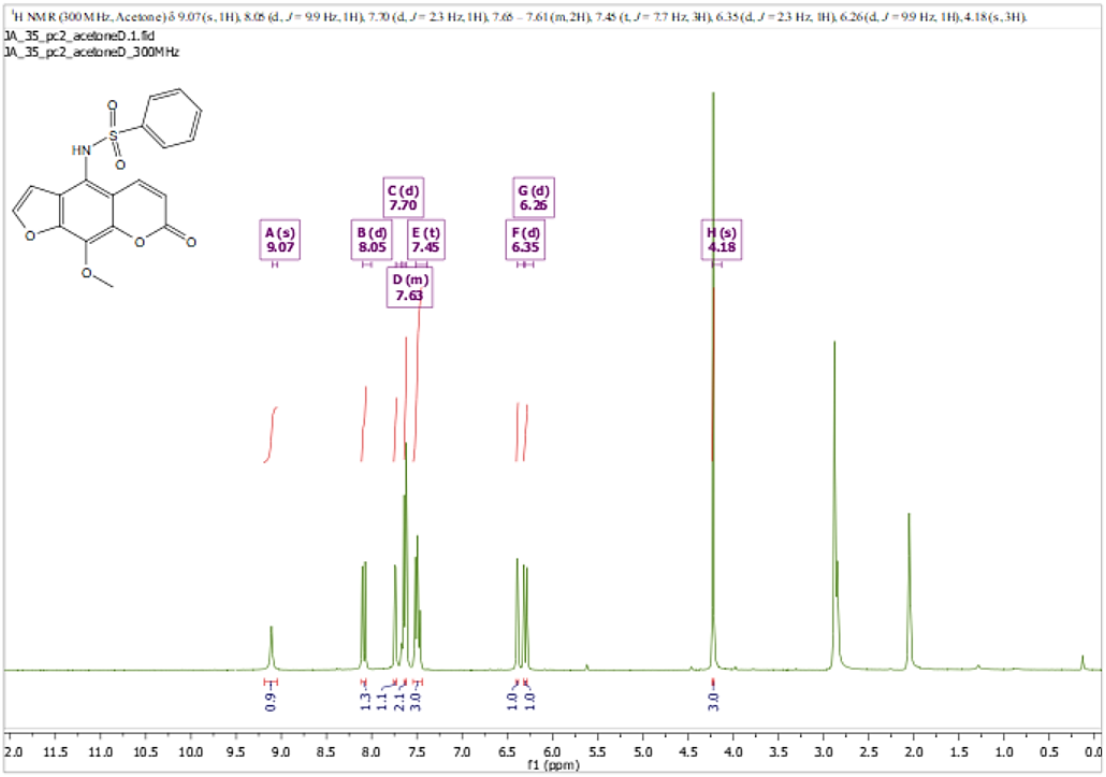

Figure S63 ^{1}H NMR spectrum of **5**

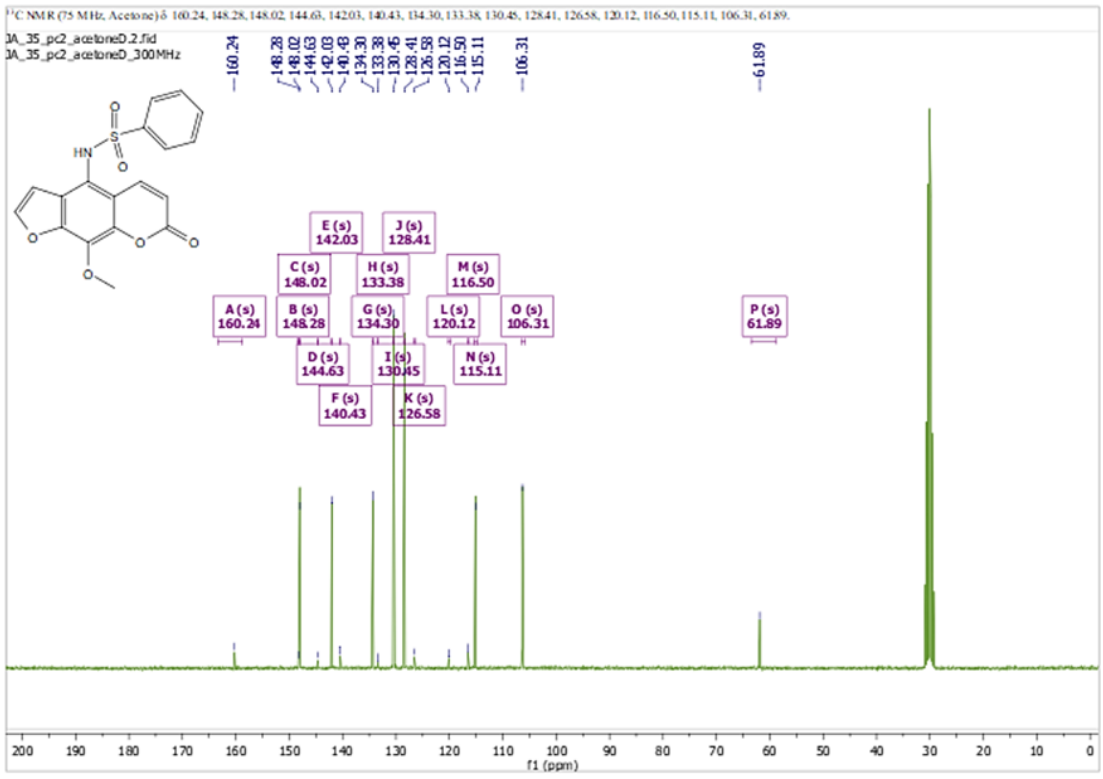

Figure S64 ^{13}C NMR spectrum of **5**

Mass Spectrum List Report

Analysis Info

Analysis Name	TOFCRI25770 Jutatip JAA36-PC2 E+.d	Acquisition Date	12/23/2019 1:34:51 AM
Method	Nitirat ESI pos 2019-1.m	Operator	Administrator
Sample Name	ESIpos	Instrument	micrOTOF 74

Acquisition Parameter

Source Type	ESI	Ion Polarity	Positive	Set Corrector Fill	64 V
Scan Range	n/a	Capillary Exit	110.0 V	Set Pulsar Pull	405 V
Scan Begin	100 m/z	Hexapole RF	160.0 V	Set Pulsar Push	405 V
Scan End	850 m/z	Skimmer 1	33.0 V	Set Reflector	1300 V
		Hexapole 1	22.9 V	Set Flight Tube	9000 V
				Set Detector TOF	1988 V

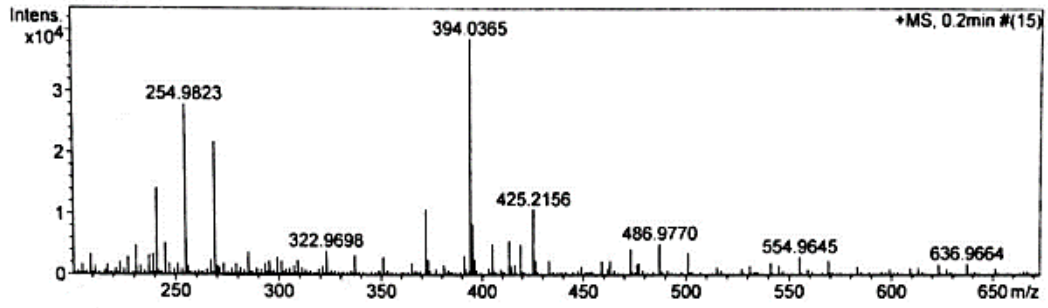

Figure S65 HRMS spectrum of **5**

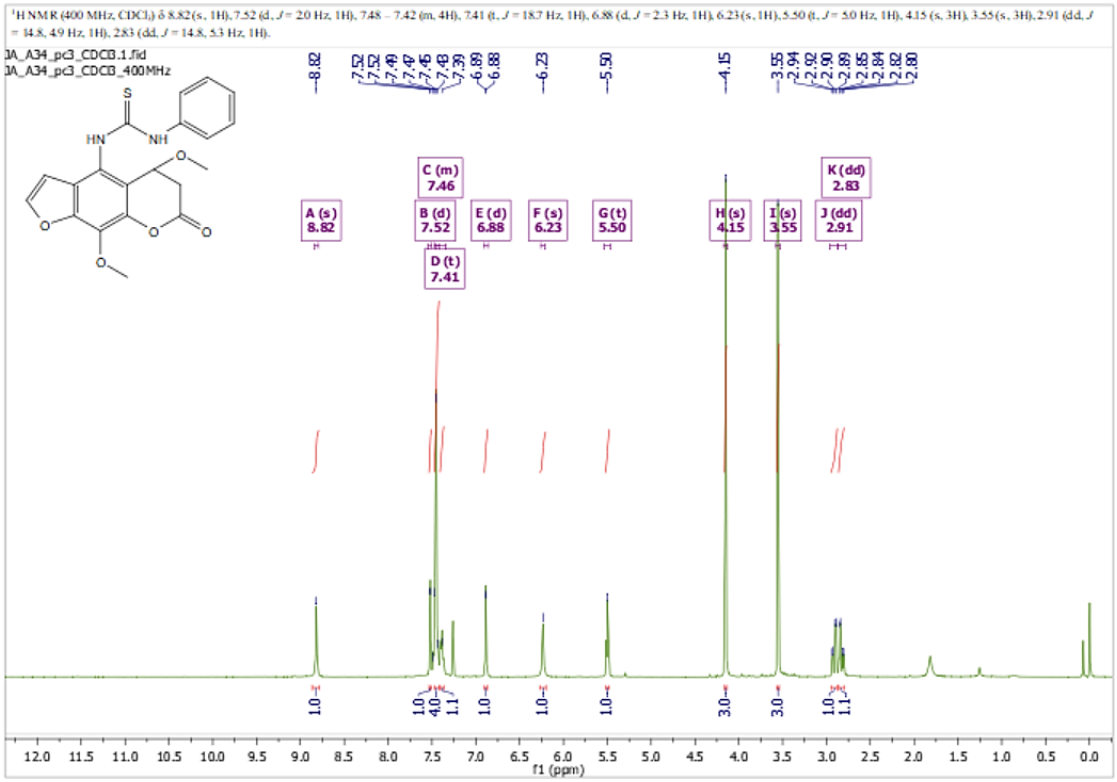

Figure S66 ^{1}H NMR spectrum of **6**

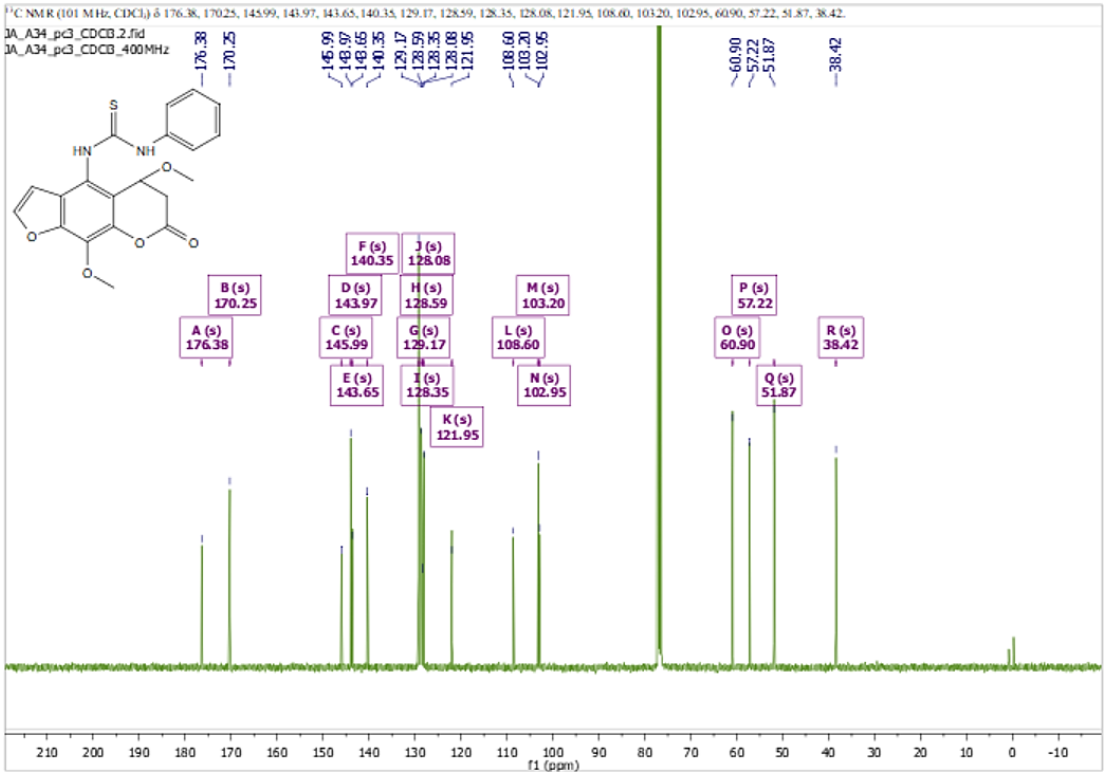

Figure S67 ^{13}C NMR spectrum of **6**

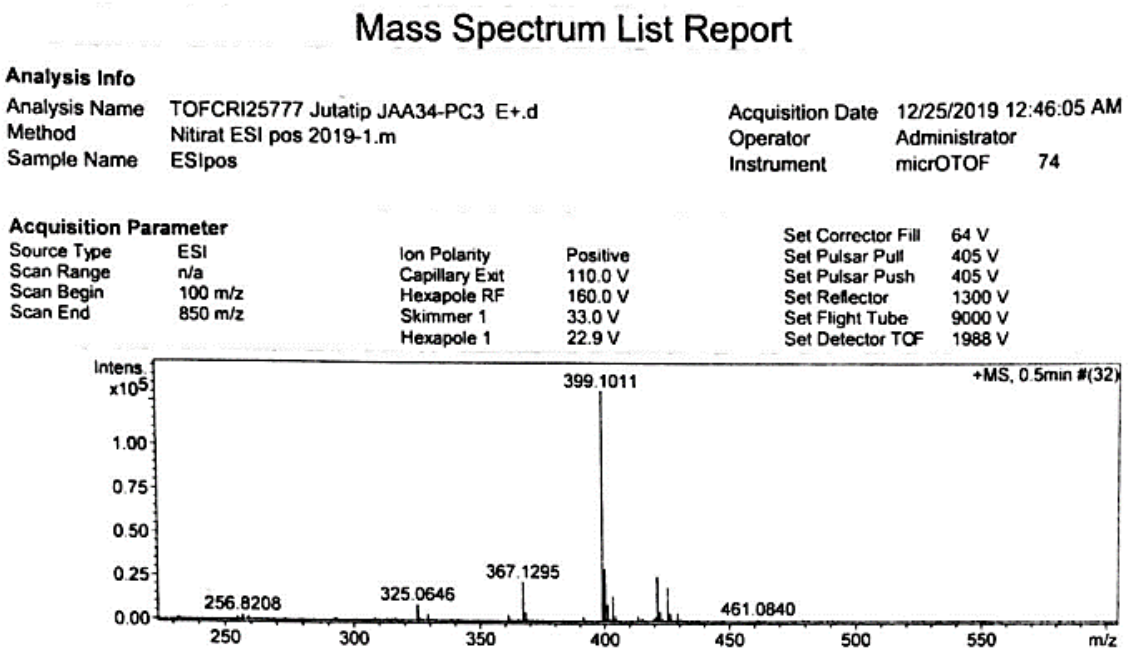

Figure S68 HRMS spectrum of **6**

5. References

[i] van Amsterdam, F. T. M., Roveri, A., Maiorino, M., Ratti, E. & Ursini, F. Lacidipine: A Dihydropyridine Calcium Antagonist with Antioxidant Activity. *Free Radic. Biol. Med.* **12**, 183–187. https://doi.org/10.1016/0891-5849(92)90025-c (1992).

[ii] Gerhäuser, C. *el at*. Mechanism-based *in vitro* Screening of Potential Cancer Chemopreventive Agents. *Mutat. Res.* **523–524**, 163–172. https://doi.org/10.1016/S0027-5107(02)00332-9 (2003).

[iii] Rangkadilok, N. *el at*. Evaluation of Free Radical Scavenging and Antityrosinase Activities of Standardized Longan Fruit Extract. *Food Chem. Toxicol.* **45**, 328–336. https://doi.org/10.1016/j.fct.2006.08.022 (2007).

[iv] Gleason, M.M., Rojas, C.J., Learn, K.S., Perrone, M.H. & Bilder, G.E. Characterization and Inhibition of 15-lipoxygenase in Human Monocytes: Comparison with Soybean 15-lipoxygenase. *Am. J. Physiol.* **268**, C1301–C1307. https://doi.org/10.1152/ajpcell.1995.268.5.c1301 (1995).